

# FERMILAB-Proposal-0641

April 23, 1980

Scientific Spokesman: T. Kitagaki  
Bubble Chamber Physics Lab  
Tohoku University  
Sendai 980  
Japan  
Tel: (022) 22-1828 x5628

Alternate Spokesman: J. Schneps  
Physics Dept.  
Tufts University  
Medford, MA 02155  
Tel: (617)-628-5000 x241

A TEVATRON PROPOSAL: NEUTRINO-DEUTERIUM AND ANTINEUTRINO-DEUTERIUM  
INTERACTIONS IN THE 15-FOOT BUBBLE CHAMBER USING AN 800 - 1000 GeV/c  
QUADRUPOLE TRIFLET BEAM.

R.A. Burnstein, J. Hanlon and H.A. Rubin  
Illinois Institute of Technology, Chicago, IL 60616

C.Y. Chang, T.W. Dombeck, B. Sechi-Zorn, G.A. Snow, P.H. Steinberg and M. Zieminska  
University of Maryland, College Park, MD 20742

S. Yamashita, N. Fujiwara and S. Noguchi  
Nara Women's University, Nara, Japan

T. Kitagaki, S. Tanaka, H. Yuta, K. Abe, K. Hasegawa, A. Yamaguchi, K. Tamai,  
T. Hayashino, S. Kunori, Y. Ohtani and M. Hayano  
Tohoku University, Sendai 980, Japan

M. Higuchi and M. Sato  
Tohoku Gakuin University, Sendai, Japan

W.A. Mann, A. Napier, J. Schneps and H. Wald  
Tufts University, Medford, MA 02155

## SUMMARY

We propose a neutrino-deuterium experiment at Tevatron energies, 800-1000 GeV, in the 15-foot bubble chamber using the Quadrupole Triplet Beam. We request  $2 \times 10^{18}$  protons on target, corresponding to 200,000 pictures with  $10^{13}$  protons per pulse. This proposal is submitted by the E545 collaboration, and is intended to continue our program of study of all aspects of neutrino and anti-neutrino interactions on neutrons and protons at higher energies. Moreover, the use of the Quadrupole Triplet Beam enables us to carry out an "ideal experiment" namely a comparison between neutrino and antineutrino interactions on neutrons and protons in the same beam and with the same analysis. It is obvious that these higher energies, which the Tevatron provides, make it possible to observe a much wider range in the variables  $Q^2$  and  $W$  and hence to explore the new phenomena in structure functions and fragmentation processes related to QCD. In addition, higher energy neutrinos and antineutrinos will produce higher momentum short lived particles - such as charmed and bottom (and top) - and with additional experimental features we expect to identify them more effectively.

Besides the EMI, the new features we are requesting in this experiment are the following: an internal picket fence extended to  $360^\circ$ ; a two-plate system inside the chamber for identifying  $\gamma$ 's and  $e^\pm$ ; and high resolution optics to search for short decay tracks and examine vertices closely.

## TABLE OF CONTENTS

	PAGE
I. INTRODUCTION - - - - -	1
II. PHYSICS - - - - -	3
A. Charged Current Physics - - - - -	3
a. Structure Functions - - - - -	3
b. Properties of Final State Hadrons in Charged Current Interactions - - - - -	4
1) Multiplicities - - - - -	5
2) Separation of current and target fragmentation regions	6
3) Fragmentation functions - - - - -	7
4) Transverse momentum distributions - - - - -	8
5) Jets - - - - -	8
6) Strange particles - - - - -	9
7) Net charge in the current fragmentation region - - -	10
8) Pion structure function - - - - -	12
9) Other topics - - - - -	13
B. Production of New Particles - - - - -	14
C. Neutral Currents - - - - -	15
III. EXPERIMENT - - - - -	17
A. Proposal - - - - -	17
B. Beam - - - - -	19
C. Separation of $\nu_{\mu}$ and $\bar{\nu}_{\mu}$ Events - - - - -	21
D. Plates - - - - -	22
E. High Resolution Optics - - - - -	24
F. EMI and IPF - - - - -	25
G. Data Reduction - - - - -	25
References - - - - -	26
Figure Captions - - - - -	28
Appendix A: Detection of Neutrino Produced Photons and Electrons by Plates - - - - -	34
Appendix B: Summary of Progress in E-545 - - - - -	51

## I. INTRODUCTION

This Tevatron proposal is submitted by the collaboration which is carrying out E-545, neutrino interactions in deuterium in the 15-foot bubble chamber using the 350 GeV/c wide band beam. In a recently submitted proposal<sup>\*</sup> we have reviewed the progress of E-545 to date (included here as Appendix B) and requested an extension at 400 GeV/c with the addition of plates and high resolution optics to the chamber. The present proposal is a request to continue our program of study of all aspects of neutrino-deuterium and antineutrino-deuterium interactions at higher energies, namely in the 800-1000 GeV/c Quadrupole Triplet Beam. We again wish plates and high resolution optics for the chamber, the present two plane EMI and the Internal Picket Fence. An extension of the IPF to cover 360° would be desirable in order to reduce neutral hadronic background originating in upstream neutrino interactions.

The primary advantage of the Tevatron beam is in the substantial increase of high energy neutrinos and antineutrinos it produces. This makes it possible to observe a much wider range in the variables  $Q^2$  and  $W$  and hence to more effectively test QCD in structure functions and fragmentation processes. In addition higher energy neutrinos and antineutrinos will produce higher momentum short lived particles - for example, charmed and bottom - and the decay tracks of some of these particles would be observed

Once again we emphasize the use of deuterium as the favored light liquid. Not only can both neutron and proton processes be studied simultaneously, but differences in their cross sections, that is, flavor non-singlet cross

\* Proposal for an Extension of E-545 to Study Neutrino Interactions in Deuterium in the 15-foot Bubble Chamber with Plates and High Resolution Optics Using the 400 GeV/c Wide Band Beam.

sections, can be obtained because the incident flux is the same for both n and p. At these higher energies the ocean quarks contribute more importantly to the total cross section and it will be of great interest to search for differences in the number of ocean  $d\bar{d}$  pairs in  $\nu n$  and  $\nu p$ , as has been suggested by  $e_n$ - $e_p$  data<sup>(1)</sup>, as well as to measure QCD effects on the ocean. In addition the strong correlation of  $K^0$  production with ocean quark targets ( $s \rightarrow c$ ) at small  $x$  can be exploited to study  $s\bar{s}$  densities as a function of  $Q^2$ .

In this experiment we shall be able to separate the neutrino and anti-neutrino interactions as well as to separate neutron and proton events. This measurement of both  $\nu n$ ,  $\nu p$  and  $\bar{\nu} n$ ,  $\bar{\nu} p$  in the same beam and under the same conditions of analysis constitutes an ideal experiment.

We request  $2 \times 10^{18}$  protons on target using the Quadrupole Triplet Beam in the deuterium filled 15-foot bubble chamber with two plates, high resolution optics, the EMI and IPF.

The physics justification and the questions of beam, plates, high resolution optics and event rates are discussed in the following sections.

## II. PHYSICS

### A. CHARGED CURRENT PHYSICS

#### a. Structure Functions

QCD predicts how the structure functions deviate from scaling, that is how they depend on  $Q^2$ . In the present regime of neutrino energies,  $Q^2$  up to  $100 \text{ GeV}^2$ , it has proven impossible to separate the leading-order QCD effects from corrections coming from non-leading higher twist terms which may contribute 0-100% of the deviation. For a non-singlet structure function, such as  $F^P - F^N$ , these effects may be expressed in terms of the moments defined by  $M_N(Q^2) = \int_0^1 dx x^{N-1} F(x, Q^2)$ . According to QCD (2)

$$M_N(Q^2) = \frac{A_N}{(\ln Q^2/\Lambda^2)^{d_N}} \left\{ 1 + \sum_{i=1}^{\infty} B_{iN} \ln(Q^2/\Lambda^2) \left[ \frac{\ln(Q^2/\Lambda^2)}{Q^2} \right]^i + \text{higher order perturbation terms} \right\}$$

The higher twist effects appear in the sum and are  $\propto [1/Q^2]^i$ . If it is going to be possible to separate these effects it will be necessary to examine the structure functions over a wide range of  $Q^2$ . By going to Tevatron energies we will be able to extend the studies of deviations from scaling over a range of  $Q^2$  values up to  $200 \text{ GeV}^2$ . In addition, by using deuterium we can study the flavor non-singlet structure function, thus eliminating the effects of gluon and sea quark distributions in the nucleon. These studies would be carried out using the CC antineutrino interactions found in this film together with the more abundant neutrino events.

In principle, in order to determine  $x$  and  $Q^2$  precisely, one should know the momentum of the neutral hadrons. Although the proposed plates will detect  $\pi^0$ 's, we do not expect to be able to measure their energy well, and of course neutrons and  $K_L^0$  will not be detected. Therefore the usual method for correcting

for neutral momentum will be used; that is to use momentum balance to determine the component transverse to the beam direction, and then choosing the longitudinal component so that the total neutral momentum will be in the same direction as the total charged hadron momentum. The plates, however, could prove useful in checking the validity of such a procedure. For example, the angular distribution of photons from  $\pi^0$  decay with respect to the charged hadron momentum axis could be studied as could  $\pi^0$  multiplicities as a function of neutral hadron energy.

To test for asymmetries between  $u\bar{u}$  and  $d\bar{d}$  in the proton or neutron, one can use the relation

$$\bar{u} - \bar{d} = \frac{3}{2} (F_2^{e(\mu)p} - F_2^{e(\mu)n}) - \frac{1}{4} (F_2^{\nu n} - F_2^{\nu p})$$

where  $\bar{u}$  and  $\bar{d}$  are the corresponding quark parton densities in the proton ( $\bar{u}_p = \bar{d}_n = \bar{u}$ ). Such an analysis at high energies (and small  $x$ ) will be able to confirm the hints from low energy  $ed$  and  $ep$  experiments that  $\bar{u}$  is less than  $\bar{d}$  by amounts much larger than is predicted at high energies by QCD<sup>(3)</sup>.

b. Properties of Final State Hadrons in Charged Current Interactions.

The bubble chamber, because of its  $4\pi$  acceptance and the ability to measure individual tracks in it, is a most suitable tool for obtaining detailed information on the hadronic final states in  $\nu$  and  $\bar{\nu}$  CC interactions. In addition the analysis is simplified for these reactions because we are primarily observing, in the current fragmentation region, the fragmentation of  $u$  and  $d$  quarks respectively, and in the target fragmentation region, the fragmentation of a spectator diquark. Such processes can be studied in terms of the quark-parton model and deviations from the scaling behavior

predicted by it can be used as tests of QCD. Of course there are complicating factors. On the experimental side, although individual tracks may be measured they cannot usually be identified unless they are slow. Thus fragmentation functions for  $K^+$ ,  $K^-$  and  $p$  are difficult to obtain, as is also the case for neutral particles. Furthermore, the fact that  $\nu$  and  $\bar{\nu}$  may scatter from sea quarks and diquarks, that they may produce  $c$  and  $s$  quarks (even  $t$  and  $b$  quarks) as well as  $u$  and  $d$  quarks, that higher twist terms may contribute, complicates the analysis. The proposed experiment can help unravel some of these competing factors. A study of  $\Lambda^0$  and  $\Sigma^0$  production in the forward hemisphere as a function of  $Q^2$  can set limits on the higher twist contributions. The  $K^0$  and  $\bar{K}^0$ 's produced in small  $x$  collisions are a good monitor of  $s \rightarrow c$  and  $\bar{s} \rightarrow \bar{c}$  transitions respectively. A study of neutron minus proton,  $(n-p)$ , fragmentation functions for  $\nu$  and  $\bar{\nu}$  can isolate non-singlet terms and eliminate strange and charm complications.

A great deal of work has already been done at present energies in studying the final hadronic state.<sup>(4)</sup> Nevertheless it has become clear that in order to answer the pressing questions, particularly concerning QCD, it is necessary to expand the range of values of  $Q^2$ ,  $W$  and  $p_T^2$  which can be examined, and to obtain some independent estimate of higher twist effects in the observed reactions.

In the remainder of this section we discuss a variety of topics concerning the hadronic final state which we intend to study.

### 1) Multiplicities

Multiplicity distributions for charged hadrons, as well as average multiplicity and dispersion have been studied as a function of  $W$  for  $\nu p$  and  $\bar{\nu} p$  CC reactions.<sup>(5)</sup> There is no apparent  $Q^2$  dependence, and the average multiplicity tends to increase linearly with  $W^2$ . KNO scaling also is approximately

satisfied. These properties have now been studied for  $\nu n$  as well as  $\nu p$  in E-545. In this experiment we would extend these investigations over the broader range of  $W$  and  $Q^2$  made available by the Tevatron for both  $\nu$  and  $\bar{\nu}$  on both  $n$  and  $p$ , which will enable us to answer questions such as the following: Does the average charge multiplicity grow faster than  $\ln s$  as has been recently observed for  $e^+e^-$  collisions? Does the ratio  $D/\langle n_c \rangle$  increase at higher  $W$  and  $Q^2$  as suggested by QCD<sup>(6)</sup>?

## 2) Separation of Current and Target Fragmentation Regions.

It has been shown<sup>(7)</sup> that by using rapidity distributions or  $x_F$  distributions in the hadron center of mass system or by appropriate choice of forward hadrons in the Breit system, reasonable separation of current and target fragmentation regions can be obtained provided cuts of  $W > 4.0$  GeV and  $Q^2 > 1$  GeV<sup>2</sup> are used. With presently available neutrino beams these are severe cuts which eliminate a substantial fraction of the events. With the higher range of  $W$  available from the Tevatron beams, not only will the fraction of events cut be reduced, but the separation into target and fragmentation regions will be improved because of the greater range in rapidity ( $\Delta y \sim \ln W^2$ ). Thus a cleaner study of fragmentation functions and charge distributions will be possible. Recent phenomenological theories<sup>(8)</sup> successfully describe the bulk of strong interaction reactions in terms of a two sheet structure, where each sheet consists of a multiperipheral chain generated by a quark and a diquark. Obtaining more precise diquark fragmentation functions from  $n$  and  $p$  targets struck by neutrinos, can refine these predictions and correlations considerably.

3) Fragmentation Functions

In general, for  $\nu$  charged current scattering the cross section may be written

$$\frac{d^3 \sigma}{dx dQ^2 dz} = \frac{d\sigma}{dx dQ^2} \cdot D^h(x, Q^2, z)$$

where  $D^h(x, Q^2, z)$  is called the fragmentation function into hadrons and  $d\sigma/dx dQ^2$  is the event cross section;  $z$  is  $E_h/E_H$  where  $E_H$  is the energy of all hadrons in the lab system. In the simple quark-parton model, the fragmentation function satisfies the properties of factorization,  $D^h(x, Q^2, z) = D^h(Q^2, z)$ , and scaling,  $D^h(Q^2, z) = D^h(z)$ . If one chooses only forward hadrons, say in the hadron center of mass, then  $D^h(z)$  may be interpreted as  $D_u^h(z)$ , the fragmentation function for the u-quark (d-quark for  $\bar{\nu}$  reactions).

QCD predicts, because of gluon processes, that the D-functions will have a  $Q^2$  dependence. Comparisons of these functions with QCD are facilitated by the use of their moments defined by

$$D(m, Q^2) = \int_c^1 z^{m-1} D(z, Q^2) dz$$

Non-singlet moments,  $D^{NS} = D^+ - D^-$ , have a particularly simple form as a function of  $Q^2$  such that a plot of one moment vs. another on a log-log scale will be a straight line.

A variety of studies of fragmentation functions and their moments have been and are being carried out at present day energies <sup>(9)</sup> testing factorization, scaling and QCD predictions. There is reasonable agreement with QCD but nevertheless it is very important to go to higher neutrino energies, and higher  $Q^2$ , to make these tests more reliable and more informative. Studying these processes for the non singlet combination ( $\nu n - \nu p$ ) makes the comparison between theory and experiment substantially cleaner. <sup>(10)</sup>

4) Transverse Momentum Distributions

QCD predicts that single hadrons arising from the hadronization of the struck quark will acquire transverse momentum due to gluon bremsstrahlung. The situation is complicated by other sources of transverse momentum, namely the primordial transverse momentum of the original quark in the nucleon, and a transverse momentum arising in the fragmentation. Altarelli<sup>(11)</sup> predicts  $k_T^2(\text{QCD}) \propto W^2 / \ln(Q^2/\lambda^2)$  for the QCD contribution. Present studies have shown some qualitative though not quantitative agreement with QCD;  $Q^2$  and  $W^2$  dependences are seen, particularly at high  $z$ . It is clear that a higher range of  $W^2$  and  $Q^2$  will do much to clarify the situation. Again,  $(\nu_n - \nu_p)$  as well as  $(\nu_n + \nu_p)$  analyses are useful.

5) Jets

Jet analyses may be carried out in terms of the usual quantities - sphericity, sphericity and thrust. In the quark-parton model one expects, in the hadron center of mass, back to back jets arising from the hadronization of the struck quark and recoiling diquark. At sufficient hadronic energy,  $W$ , according to 1st order QCD a third jet should arise from gluon emission. At presently available values of  $W$ ,  $\lesssim 15$  GeV, no such effects are seen and even if present would probably be washed out by non-QCD effects. It will thus be very interesting to perform this type of analysis with the higher  $W$  available at Tevatron energies, although even here it will probably not be high enough to allow as clean analyses as at PETRA or PEP. On the other hand, in high energy neutrino interactions one can study and compare diquark jets with single quark jets, which should be interesting.<sup>(12)</sup>

6) Strange Particles

Although it will not be possible to achieve good identification of charged strange particles in this experiment, a great deal can be learned from neutral strange particle production. In E-545 we have found a rate of about 19% for the production of  $V^0$ 's from deuterium in neutrino interactions - 13%  $K^0$ ,  $\bar{K}^0$ ; 6%  $\Lambda^0$ ; and 0.2%  $\bar{\Lambda}^0$ .

It is now apparent that charmed particle production is of the order of 5-10% in neutrino interactions, of which the charmed baryon part may be as low as 1%. Thus the expected  $\bar{K}^0$  rate from charm will be about 3-4% and the  $\Lambda^0$  rate only a few tenths of a percent. It is evident that most of the strange particles arise from the fragmentation of the forward u quark and the recoiling diquark.

If the quark sea is SU2 symmetric ( $\gamma_u = \gamma_d$ ) then we would expect in the u-quark fragmentation that

$$\frac{N_{K^0} + N_{\bar{K}^0}}{N_{\pi^+} + N_{\pi^-}} \approx \frac{\gamma_s}{\gamma_u}$$

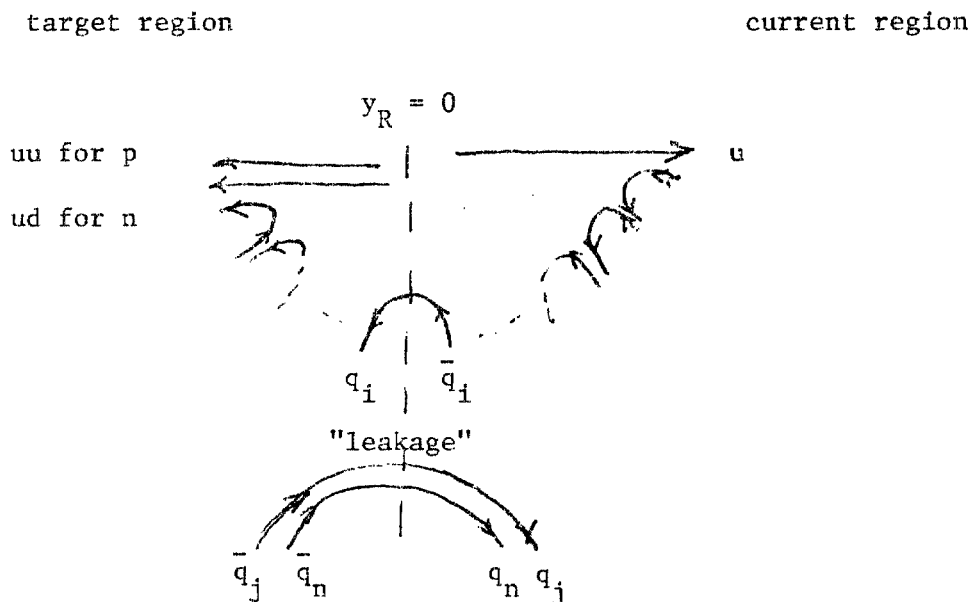
which is an independent method from that of the net forward charge (section 7) to determine  $\gamma_s$ . As pointed out before, with a higher range of W available this determination will become more reliable.

The  $\Lambda^0$  production is of particular interest in that the  $\Lambda^0$  is the only baryon which we can identify over its entire momentum spectrum. As shown by our rapidity distribution for  $\Lambda^0$ 's, the largest part of them arise from the backward moving diquark (in the hadron CM).  $\Lambda^0$ 's which arise from gluon  $\Lambda \bar{\Lambda}$  pair creation are expected to cluster in the central region, about  $y = 0$ , and their number can be estimated from the number of  $\bar{\Lambda}^0$ 's. Forward  $\Lambda^0$ 's may arise in two ways: first, from fragmentation of the emerging u or c quark

and second, from a higher twist effect, the  $\nu$  scattering from a diquark<sup>(13)</sup>, which is expected to go as  $1/Q^4$ . In addition, the production of a  $\Lambda^0$  from a struck diquark should take place primarily from neutrons and not from protons, since the required process is  $\nu + (dd) \rightarrow (ud)$  with the  $(ud)$  picking up a strange quark in the hadronization process to form a  $\Lambda^0$ . In terms of valence quarks, the  $dd$  of course only exists in the neutron. In view of this, it would be interesting to have a  $Q^2$  and  $W$  range large enough so that one could examine forward  $\Lambda$  production in a high and a low  $Q^2$  region, comparing this for neutrons versus protons. It is important that the range of  $W$  available be large enough so that any observed  $Q^2$  effects cannot be attributed to phase space restrictions due to limitations on the magnitude of  $W$  available. With the two plates in the chamber we have a substantial probability of detecting the  $\gamma$  from forwardly produced  $\Sigma^0$ 's ( $\Sigma^0 \rightarrow \Lambda + \gamma$ ). Hence, if diquark absorption does occur we will be able to compare  $(ud) \rightarrow \Lambda$  with  $(ud) \rightarrow \Sigma^0$ , thus learning something about the relative amounts of  $I = 1, S = 1$   $(ud)$  diquarks (needed for  $\Sigma^0$ ) and  $I = 0, S = 0$   $(ud)$  diquarks (needed for  $\Lambda$ ).<sup>(14)</sup> This field of study is uniquely suited to a  $\nu$ - $D_2$  exposure.

### 7) Net Charge in the Current Fragmentation Region

In neutrino interactions, the net charge in the current fragmentation region is not a measure of the charge of the  $u$  quark ( $d$  quark for  $\bar{\nu}$  interactions) but only a measure of the probability  $\gamma_u$  of producing a  $u\bar{u}$  pair from the sea as illustrated in the diagram below.



The net forward charge will be

$$\langle Q_F \rangle = e_u - \sum_i \gamma_i e_i \quad i = u, d, s$$

where  $e_i$  is the charge of quark  $q_i$ ,  $\gamma_i$  is the probability of producing a pair  $q_i \bar{q}_i$  from the sea,  $\sum_i \gamma_i e_i$  is the "leakage" term, and

$$\gamma_u + \gamma_d + \gamma_s = 1 \quad \text{or} \quad \gamma_d + \gamma_s = 1 - \gamma_u.$$

$$\text{Then } \langle Q_F \rangle = \frac{2}{3} - \left[ \frac{2}{3} \gamma_u - \frac{1}{3} \gamma_d - \frac{1}{3} \gamma_s \right] = \frac{2}{3} - \frac{2}{3} \gamma_u + \frac{1}{3} (\gamma_d + \gamma_s) = 1 - \gamma_u.$$

Furthermore if we assume  $\gamma_u = \gamma_d$  then  $\gamma_s = 1 - 2\gamma_u$ .

As well as the leakage of a single quark out of the forward charge region we may also consider the smaller effect of the leakage of a diquark into the forward region. Then

$$\langle Q_F \rangle = e_u - \sum \gamma_i e_i + \sum \Gamma_{jk} (e_j + e_u)$$

where we may define

$$x = \Gamma_{uu} + \Gamma_{ud} + \Gamma_{us} + \Gamma_{dd} + \Gamma_{ds} + \Gamma_{ss}$$

and

$$\gamma_u + \gamma_d + \gamma_s + x = 1.$$

Then

$$\langle Q_F \rangle = 1 - \gamma_u + \Gamma$$

where

$$\Gamma = \Gamma_{uu} - \Gamma_{dd} - \Gamma_{us} - \Gamma_{ss}.$$

For antineutrinos we find

$$\langle \bar{Q}_F \rangle = -\gamma_u \text{ in the case of only single quark leakage, and}$$

$$\langle \bar{Q}_F \rangle = -\gamma_u + \Gamma \text{ if diquark leakage is also included.}$$

The question remains as to how to determine the true value of  $\langle Q_F \rangle$ . First one should prefer large  $x$  to minimize the contributions of scattering from sea quarks. Even so, there is still difficulty because at finite  $W$  there is overlap between the current and target fragmentation regions. One approach is to extrapolate to  $W = \infty$ , which is done by extrapolating  $1/W$  to zero linearly. Since the largest  $W$  values used are about 10 GeV it is clear that the reliability of the measurements of  $\langle Q_F \rangle$  and  $\langle \bar{Q}_F \rangle$  could benefit greatly by extending the  $W$  range available. We have already observed interesting differences in the exchanged charge for  $K^0$  and  $\Lambda^0$  events as compared to non strange particle events. These studies can be improved and extended.

### 8) Pion Structure Function

The pion form factor can be determined from events of the type  $\nu + n \rightarrow p + X$  where the neutron dissociates into  $p\pi^-$  and the neutrino

strikes the virtual  $\pi^-$  leaving a visible proton in the momentum region 400-800 MeV/c. The effect, as described by Lusignoli et. al. <sup>(15)</sup> is much larger and easier to detect with  $E_\nu > 100$  GeV than at lower neutrino energies. This method of determining pion form factors is straightforward and completely different from the Drell-Yan method that seems to be very sensitive to higher order QCD corrections. It should be very interesting to compare the results for the two methods. About 200-300 events of this type are expected in the proposed run.

#### 9) Other Topics

Some additional topics of interest are the following:

- The study of exclusive channels such as

$$\nu n \rightarrow \mu^- p, \mu^- \Lambda^0 K^+, \text{ etc.}$$

$$\nu p \rightarrow \mu^- p \pi^+, \mu^- p K^+, \text{ etc.}$$

can be extended to higher energies.

- The current production of vector and axial vector mesons can be measured.
- The Adler sum rule can be pushed to lower x-values.
- Meson and baryon resonance production, both strange and non-strange, will be studied over a wider range of W.
- Inclusive  $\Delta^{++}$  production,  $\nu D \rightarrow \mu^- \Delta^{++} + X$ , can be studied. In particular, a study of low momentum spectator  $\Delta^{++}$  can yield an estimate of the fraction of the deuteron wave function in which a  $\Delta^{++}$  is present -- a quantity of considerable interest to nuclear physicists. Using higher energy neutrinos for this study increases the separation between spectator  $\Delta^{++}$  and  $\Delta^{++}$  that are produced in ordinary  $\nu p$  collisions.

## B. PRODUCTION OF NEW PARTICLES

By new particles, we refer to charmed particles,  $\tau$ -leptons, and particles containing bottom or top quarks. With plates and high resolution optics it will be possible to obtain considerable information on charmed particle production in neutrino interactions. The number of charmed particles estimated to be produced in the proposed neutrino experiment is  $\sim 1400$ . With the proposed 200 micron resolution optics, covering about 1/3 the available fiducial volume, about 90 should be seen to decay. In addition, the plates will make it possible to pick up the leptonic decays of charmed particles into  $e^\pm$ . The comparison of  $e^\pm$  produced from visible charmed decays with overall  $e^\pm$  production will enable us to obtain useful information on background sources of  $e^\pm$ .

In addition to the detection of  $e^\pm$  from charm decays the plates will also make possible the detection of  $\pi^0$ 's from these decays. As we have pointed out in a recently submitted 400 GeV/c proposal, the number of  $\nu$  events with charm which can be fit exclusively will increase with  $\pi^0$  detection in the plates.

The detection of charm in the  $\bar{\nu}$  events would be a measure of the amount of hadronization of charm from the sea,  $\gamma_c$ , and would also allow us to more precisely sort the sea production from direct charm production in  $\nu$  interactions.

The expected production of  $F^+$  mesons is about 150, of which  $\sim 1/3$  would be in the high resolution region.

In the case of the production of a bottom particle in an antineutrino interaction followed by the successive decays  $b \rightarrow c \rightarrow s$  the characteristic zigzag could be seen provided that the b lifetime is long enough. In fact the b lifetime has been predicted to be comparable to the charm lifetime,  $\sim 10^{-13}$  sec.,<sup>(16)</sup> so that at higher energies their decays could be seen with HRO. Using predicted cross sections for b production<sup>(17)</sup> we find  $\sim 5$  bottom particles would be produced in this exposure. The probability of observing visible decays then is very small; on the other hand even a few examples could be quite convincing.

Preliminary results at CERN and Fermilab suggest a mass bump in the 5-6 GeV region from  $\bar{\nu}$  events giving rise to  $\mu^+ \ell^-$ . If real this would suggest a rather large cross section for single bottom events which could lead to interesting information about bottom production even in this proposed  $D_2$  run.

### G. NEUTRAL CURRENTS

The study of neutral currents in this proposed experiment would be enhanced in comparison to earlier lower energy experiments by a reduction in the contamination of the NC event sample. We would expect that at higher neutrino energies the contribution to background by both CC events with slow muons and events produced by neutral hadrons would be reduced. In addition,

if the IPF were extended to  $360^\circ$  the neutral hadron background would be further reduced. Together with this the increased number of events at higher energies would also make it possible to more accurately determine the NC/CC ratios on both n and p. From this we should be able to obtain better results on  $u_L^2$ ,  $d_L^2$  and  $\sin^2\theta_W$  than could be obtained in E-545.

With the use of the plates we will be able to detect most of the  $\pi^0$ 's produced in neutral current interactions ( $\sim 60\%$ ). Thus we will be able to determine neutral pion multiplicities from neutral current events. In addition, we note that the detected  $\pi^0$ 's tend to be the fast forward ones and thus carry an even greater percentage of the neutral hadronic energy in pions. Although we do not expect to be able to measure the individual  $\pi^0$  energies well in the plates we may be able to make a rough estimate of the neutral hadronic energy. We cannot be sure at this time how valid any such procedure would be, but in any case, it will be easy to check the validity of the procedure by applying it to the CC events and comparing it with the method presently used to estimate neutral energy, the so-called "Bonn" method described earlier. If the method does prove valid we can then obtain in a given event an estimate of the energy of the incoming neutrino as well as of the momentum and direction of the outgoing neutrino. All the relevant variables  $x$ ,  $y$ ,  $Q^2$ ,  $W$  can then also be estimated and the neutral current events can be subjected to the same kinds of analysis we have already discussed for charged current events.

We would also study  $V^0$  production in NC events and contrast it with  $V^0$  production in CC events. In this way we would try to test the  $SU(2) \times U(1)$  selection rules for charm production.

### III. EXPERIMENT

#### A. Proposal

We propose a  $2 \times 10^{18}$  proton neutrino-deuterium experiment in the Fermilab 15-foot bubble chamber at Tevatron energies which would include the following features:

Beam - the Quadrupole Triplet Beam at 1000 GeV/c with 400 GeV/c tuning and  $10^{13}$  protons per pulse;

Exposure and Event Rates - We request 200,000 pictures. The event rates corresponding to this exposure are shown in Table I. If the number of protons per pulse is less than  $10^{13}$  we request correspondingly more pictures.

EMI and IPF - The two plane EMI configuration and an extended internal picket fence.

Plates - Two large stainless steel plates at the downstream end of the chamber for  $\gamma$  and  $e^+$  identification.

High Resolution Optics - we request three additional cameras, those which normally serve as backups, to be adapted for high resolution optics with 200 micron resolution.

Except for the beam, these features are similar to those in our recent proposal to extend E-545 to 400 GeV/c running. They are discussed in more detail in the following sections.

TABLE I : EVENT RATES

The event production rates for neutrino-deutrium and antineutrino-deutrium interactions are estimated for 1000 GeV,  $2 \times 10^{18}$  p runs ( $1 \times 10^{13}$  ppp and 200,000 pictures) assuming a quadrupole triplet beam and an  $11 \text{ m}^3$  fiducial volume of deuterium.

Reaction	No. of Events $E_\nu > 20 \text{ GeV}$	Reaction	No. of Events $E_\nu > 20 \text{ GeV}$
$\nu_\mu^p \rightarrow \mu^- X$	5600	$\bar{\nu}_\mu^p \rightarrow \mu^+ X$	1160
$\nu_\mu^n \rightarrow \mu^- X$	8300	$\bar{\nu}_\mu^n \rightarrow \mu^+ X$	770
$\nu_\mu^p \rightarrow \nu_\mu X$	2300	$\bar{\nu}_\mu^p \rightarrow \bar{\nu}_\mu X$	300
$\nu_\mu^n \rightarrow \nu_\mu X$	2300	$\bar{\nu}_\mu^n \rightarrow \bar{\nu}_\mu X$	300
$\nu_\mu^{\binom{p}{n}} \rightarrow \mu^- \Lambda X$	1000	$\bar{\nu}_\mu^{\binom{p}{n}} \rightarrow \mu^+ \Lambda X$	150
$\nu_\mu^{\binom{p}{n}} \rightarrow \mu^- K^0 X$	2400	$\bar{\nu}_\mu^{\binom{p}{n}} \rightarrow \mu^+ K^0 X$	340
$\nu_\mu^{\binom{p}{n}} \rightarrow \mu^- + \text{charm}$ (produced)	1400	$\bar{\nu}_\mu^{\binom{p}{n}} \rightarrow \mu^+ + \text{bottom}$	5
Seen with HRO	90		
$\nu_\mu^{\binom{p}{n}} \rightarrow \mu^- e^+ X$	80		
		$\nu \rightarrow \mu^- X$	$\bar{\nu} \rightarrow \mu^+ X$
$E_\nu > 20$		13900	1900
$20 < E_\nu < 100$		2600	600
$100 < E_\nu < 200$		4300	800
$E_\nu > 200$		7000	500

## B. BEAM

We have considered the following beams for this proposal:

1. The Quadrupole Triplet Beam (QTB) without sign selection;
2. The Single Horn focussed Wide Band Beam (SHB) with sign selection for neutrinos;
3. The Sign Selected Bare Target Beam (SSBT) for antineutrinos only.

We have used the neutrino spectra obtained by S. Mori<sup>(18)</sup> together with cross sections

$$\sigma_{CC}(\nu N) = 0.60 E \times 10^{-38} \text{ cm}^2/\text{nucleon} \quad (19)$$

$$\sigma_{CC}(\bar{\nu} N) = 0.30 E \times 10^{-38} \text{ cm}^2/\text{nucleon} \quad (20) \quad (E \text{ in GeV})$$

to obtain charged current (CC) event rates. In Fig. 1, integrated CC event rates are shown for the QTB, the SHB for neutrinos and the SSBT for antineutrinos. Also shown are the antineutrino background for the QTB and SHB and the neutrino background for the SSBT. The plotted quantity is the total number of CC events with neutrino energy greater than the value of the abscissa, in units of events per deuteron per  $10^{13}$  protons on target.

We have not considered the SHB, with or without plug, for anti-neutrino running because the softness of the spectrum yields very few high energy events and a total event rate about 15 times less than that for neutrinos.

For neutrinos we find that the SHB yields an event rate 1.7 times greater than that yielded by the QTB. On the other hand the QTB yields more high energy events. The numbers of events with  $E > 150$  GeV are about

equal for the two beams, however for  $E > 300$  GeV the event yield for the QTB is 1.6 times that for the SHB. In fact, 34% of the QTB events occur above 300 GeV, compared to 13% of the SHB events.

The antineutrino background above 150 GeV in the QTB and SHB are about 10% and 6% respectively. With the aid of the EMI, as we have already shown in E-545, we would be able to isolate and analyze the antineutrino CC events. The QTB yields a factor of 1.4 times as many antineutrino events as the SHB with  $E_{\bar{\nu}} > 300$  GeV.

For antineutrinos, the SSBT yields a clean beam with event rates slightly less than the background antineutrino event rates of the QTB and SHB. Considering that we can separate the antineutrino CC events in the QTB, we find the event rates for the SSBT far too low ( $\sim 2000$  events for a 200,000 picture exposure) to justify an extended run in this beam.

The exciting physics at the Tevatron is not at  $E_{\nu} < 100$  GeV, a region which we are currently investigating and propose to investigate further (see our 400 GeV proposal), but at the highest neutrino energies available. This, together with the "extremely good operational reliability"<sup>(18)</sup> of the QTB, necessary for the extended running envisioned, as well as the compatibility of the QTB with counter experiments, lead us to choose this beam as the one favored for our proposed  $\nu d$  experiment. Our second choice would be the neutrino SHB.

Antineutrino CC events would be studied simultaneously with neutrino events in either case. Neutral current neutrino events, with a not unreasonable overall background of 5-10% from antineutrinos, would also be studied, and this background would decrease significantly at higher energies.

### C. SEPARATION OF $\nu_{\mu}$ AND $\bar{\nu}_{\mu}$ EVENTS

In the Quadrupole Triplet Beam we expect the antineutrino "background" to be  $\sim 14\%$  of the overall neutrino event rate. If we wish to do antineutrino physics we need to know how well we can identify antineutrino events and what background contamination we can expect. We have studied this for a kinematical method of separation by a Monte Carlo simulation.

The following quantities are used in this method:

$\Sigma P_L$ , the longitudinal momentum of charged tracks with respect to the neutrino beam.

$P_T$ , the highest momentum transverse to the neutrino direction for a non-interacting negative track.

$P_{TR}$ , the momentum of the above particle transverse to the charged hadronic total momentum.

$F_{\max}(\bar{+}) = \text{Max}(p_T \cdot p_{TR} / (\Sigma p_T^2)^{1/2})$ , the track which maximizes this (- for  $\nu$ 's, + for  $\bar{\nu}$ 's) is the muon candidate.  $p_T^i$  are hadron momenta.

$\Phi(+)$ , the projected angle on a plane perpendicular to the neutrino direction of the angle between  $\vec{p}(\mu^+)$  and  $\vec{p}(\text{hadronic})$ .

Figure 2 shows the fraction of  $\nu$  and  $\bar{\nu}$  events as a function of a cut on  $\Sigma P_L$ . Figure 3 shows for neutrino events the effects of a cut on  $P_{TR}$  (greater than a value on the abscissa) for given  $\Sigma P_L$  cuts. Both the fraction of events retained and the purity are given. Fig. 4(a) shows the effect of the  $P_{TR}$  cut for antineutrino events, showing also the neutrino contamination. Fig. 4(b) shows the additional

effects on the  $\bar{\nu}_\mu$  sample of cuts on  $F_{\max}^{(+)}$  (greater than the abscissa value) and  $F_{\max}^{(-)}$  (less than the abscissa value) for given  $\Sigma P_L$  and  $\Sigma P_{TR}^{(+)}$  events. Figure 4(c), finally, shows the results of a  $\phi^{(+)}$  cut. Our conclusion is that the kinematical method with the cuts  $\Sigma P_L > 20$  GeV,  $P_{TR}^{(+)} > 3$  GeV,  $\text{Log}_{10} F_{\max}^{(+)} > 0.6$ ,  $\text{Log}_{10} F_{\max}^{(-)} < 0.8$  and  $\phi^{(+)} > 100$  degrees can identify 71% of all  $\bar{\nu}_\mu$  events with a sample purity of 84%.

By combining this kinematical method with information on muon identification from the EMI we can achieve an even higher purity of our antineutrino sample.

#### D. PLATES

In proposal P-545 we proposed a downstream set of four plates inside the 15-foot chamber. A test run of this system was not completely successful due to turbulent conditions in the regions between plates. Therefore the E-545 run took place in the bare chamber. The technical staff at Fermilab has determined that the problem could be cured by trimming back the plates about ten inches on top and bottom. In Appendix A, a detailed analysis of the photon and electron detection capabilities of the trimmed 4-plate system is given.

For this experiment, as in our proposal to extend E-545 at 400 GeV/c, we are proposing a modification of the 4-plate system, namely, that only two plates - the second and third - be used. The total radiation length would be  $1.44X_0$ . This modification is justified by the following considerations:

- i) We are convinced from experience with other plate experiments that shower multiplication would make the regions behind the 3rd

and 4th plates unusable. It will be very difficult to follow tracks through these regions. With only two plates, this would not be a serious problem.

ii) The technical difficulties which appeared in the 4-plate test would be significantly reduced with only one interplate region instead of three.

iii) The removal of the first plate will increase the usable fiducial volume from about 60% to 70% of the chamber.

iv) The reduction in photon and electron conversion efficiency is not great. Overall photon and electron conversion efficiencies will be about 60%. However, the efficiency for catching neutral energy is even greater.

v) The plates and their mounting supports already exist at Fermilab. The only modification required is the trimming of the top and bottom portions.

vi) Finally, it should be stressed that the electron identification power for this two plate system is very high ( $\sim 93\%$ ), with a small hadron contamination ( $\lesssim 10^{-3}$ ).

This is achieved by measuring the highest transverse momentum of the shower particles.

As mentioned earlier, we will use the plates primarily

- a) as a  $\pi^0$  veto to assist in fitting exclusive channels with no neutrals.
- b) to detect events where a single  $\pi^0$  is emitted which may then give a constrained fit.
- c) to detect electrons and positrons.
- d) to assist in separating  $\Sigma^0$ 's from  $\Lambda^0$ 's.

In addition, the use of plates with a light liquid such as deuterium will result in improved neutrino energy by detecting a major fraction of the neutral energy.

#### E. HIGH RESOLUTION OPTICS

Recently, tests with high resolution cameras which have taken place in LEBC (Little European Bubble Chamber) and in the SLAC 40-inch chamber have met with considerable success,<sup>(21)</sup> achieving resolutions of the order of 50 - 80 microns. It has been proposed at recent workshops on neutrino physics at Tevatron energies<sup>(22)</sup>, that the 15-foot chamber also be equipped with high resolution capability by modifying the three spare cameras. Because diffraction limited resolution and the depth of focus of a lens are intimately related, the 50 - 80 micron resolution referred to above would not be practical in a neutrino beam since the depth of focus is only a few centimeters. A reasonable goal for the 15-foot chamber would be 200 micron resolution which corresponds to a depth of focus of about 30 cm. With the three cameras focussed at different depths a region centered on the beam axis about 1 meter in depth and covering the length of the chamber could be observed. This would correspond to about 1/3 of the usual fiducial volume of the chamber.

We are of the opinion that high resolution optics is technologically and economically feasible for Tevatron running. We note that

at CERN one camera has recently been modified for high resolution and very good pictures have been obtained. (23)

As part of this proposal, we therefore request a three-camera high resolution system similar to that described. Our collaboration is prepared to lend considerable assistance to Fermilab in the design, development, and testing of the high resolution cameras.

#### F. EMI AND IPF

We propose to use the two-plane EMI configuration and an enhanced IPF (internal picket fence). We request that the present IPF with 16 drift chambers be extended to cover a full  $360^\circ$  in order to reduce contamination of neutral current events by neutral hadrons coming from upstream interactions.

#### G. DATA REDUCTION

The collaborating groups have already scanned, measured and processed the neutrino-deuterium experiment, E-545. The data processing systems now carry out geometric reconstruction in the 15-foot chamber, kinematic fitting and EMI analysis and produce the final Data Summary Tape. If our recently submitted proposal for an extension of E-545 at 400 GeV/c with plates and high resolution optics is approved, we would then, at the time of Tevatron running, have working systems and the experience to take into account the additional information from these new features.

The collaboration expects to be able to have  $\sim 40$  experienced scanners to carry out the scanning and measurement of the film. Based on our present experience with E-545, we estimate the neutrino and antineutrino charged current events would be completely processed within  $\sim 2$  years from the time of the experimental runs. Physics analysis would proceed simultaneously.

## REFERENCES

1. J. Steinberger, APS Division of Particles and Fields Conference, Montreal, 1979; R.D. Field and R.P. Feynman, Phys. Rev. D15, 2590 (1977) and references therein.
2. See for example L.F. Abbot, The QCD Phenomenology of Deep Inelastic Scattering, APS Division of Particles and Fields Conference, Montreal, 1979 (also a Brandeis University preprint) and references cited therein.
3. D.A. Ross and C.T. Sachrajda, Nucl. Phys. B149, 497 (1979).
4. For a complete list see N. Schmitz, Recent Results on the Hadronic Final State in Charged Current Neutrino and Antineutrino Interactions, Rapporteur's talk at 1979 Photon Lepton Conference at Fermilab, MPI-PAE/Exp. E1.80, 1979.
5. M. Derrick et. al. Phys. Rev. D17, 1 (1978); J.P. Berge et. al., Phys. Rev. D18, 3905 (1978); V. Ammosov et. al., Nuov. Cim. 51A, 539 (1979); J. Bell et. al., Phys. Rev. D19, 1(1979); P.C. Bosetti et. al., Nucl. Phys. B149, 13(1979); ABCMO Collaboration, reported by N. Schmitz, 1979 Photon-Lepton Conference at Fermilab (see ref. 4).
6. G.A. Snow, talk presented at Moriond Conference, March 1980; E-545 Collaboration (to be published).
7. B. Musgrave, Properties of the Hadronic System produced in Anti-neutrino Proton Interactions; see also N. Schmitz (ref. 4 above).
8. For example, see  
A. Capella et. al., Phys. Lett. 81B, 68(1979).
9. ABCMO Collaboration, see N. Schmitz (ref. 4); B. Musgrave et. al., 1979 Photon-Lepton Conf. Fermilab; M. Derrick et. al., ANL-HEP-CP-79-21; J.P. Berge et. al., Neutrino 79 at Bergen; H. Lubatti et. al., Neutrino 79 at Bergen; Y.G. Rjabov, 1979 Photon Lepton Conf. Fermilab; E-545 Collab., 1979 Photon Lepton Conf., Fermilab.

10. N. Sakai, Phys. Lett. 85B 67, (1978).
11. G. Altarelli, Proc. 13th Rencontre de Moriond, Vol. II, 395 (1978).
12. See for example:  
M. Fontannez et. al., Phys. Lett. 77B, 315 (1978).
13. I. Schmidt and R. Blankenbecler, Phys. Rev. D16, 1318 (1977);  
A. Fernandez-Pacheco et. al., Lett. Nuovo Cimento 22, 339 (1978).
14. L.F. Abbott et. al., Phys. Lett. 88B, 157 (1979).
15. M. Lusignoli et. al., Nucl. Phys. B155, 394 (1979).
16. T.G. Rizzo, Phys. Rev. D20, 706 (1979).
17. C. Baltay, Neutrino Physics at the Tevatron in the 15-foot Neon Bubble Chamber, Workshop on Tevatron Neutrino Physics, Argonne National Lab, Oct. 1979.
18. S. Mori, Fermilab Technical Memo TM-839, Dec. 1978.
19. S. Ciampolillo et. al., Phys. Lett. 84B, 281 (1979).
20. P.C. Bosetti et. al., Phys. Lett. 70B, 273 (1977); A.E. Asratyani et. al., Phys. Lett. 76B, 239 (1978).
21. Private Communication - G. Kalmus, Rutherford Laboratory.
22. L. Voyvodic, Argonne Workshop on Bubble Chamber Neutrino Physics at the Tevatron, Oct. 1979, and Fermilab Workshop on Muon and Neutrino Physics at the Tevatron, Jan. 1980.
23. Private Communication - D.R.O. Morrison, CERN.

## FIGURE CAPTIONS

- Fig. 1. Integrated charged current event rates for the quadrupole triplet beam, single horn beam for neutrinos, and sign selected bare target beam for antineutrinos.
- Fig. 2. Charged current selection for  $\nu_\mu$  and  $\bar{\nu}_\mu$  events with  $p_{TR}(+)$  greater than the cut value (abscissa) is shown. The quadrupole triplet beam with 1000 GeV/c incident protons and 400 GeV/c tuning is used.
- Fig. 3. The pass rate for  $\nu_\mu$  charged current events with  $p_{TR}$  greater than the cut value is shown for three different values of the  $\Sigma p_L$  cut. The purity of the  $\nu_\mu$  event sample is also shown.
- Fig. 4. (a) The pass rate for  $\bar{\nu}_\mu$  charged current events with  $p_{TR}(+)$  greater than the cut value, is shown for the case  $\Sigma p_L > 20$  GeV/c; using the cuts  $\Sigma p_L > 20$  GeV/c and  $p_{TR} > 3$  GeV/c we show in (b) the pass rate for  $\bar{\nu}_\mu$  CC events with  $\text{Log}_{10} F_{\text{max}}(+)$  greater than the cut value, as well as the  $\nu_\mu$  contamination, and in (c) the pass rate for  $\bar{\nu}_\mu$  CC events with  $\text{Log}_{10} F_{\text{max}}(-)$  less than the cut value, and  $\nu_\mu$  contamination.
- Fig. 5. Pass rates for  $\bar{\nu}_{CC}$ ,  $\nu_{CC}$ , and  $\nu_{NC}$  events for values of  $\phi(+)$  greater than the cut value, for events which have passed the cuts  $\Sigma p_L > 20$  GeV/c,  $p_{TR}(+) > 3$  GeV/c,  $\text{Log}_{10} F_{\text{max}}(+)$   $> 0.6$  and  $\text{Log}_{10} F_{\text{max}}(-)$   $< 0.8$ .

# INTEGRATED CHARGED CURRENT EVENT RATES

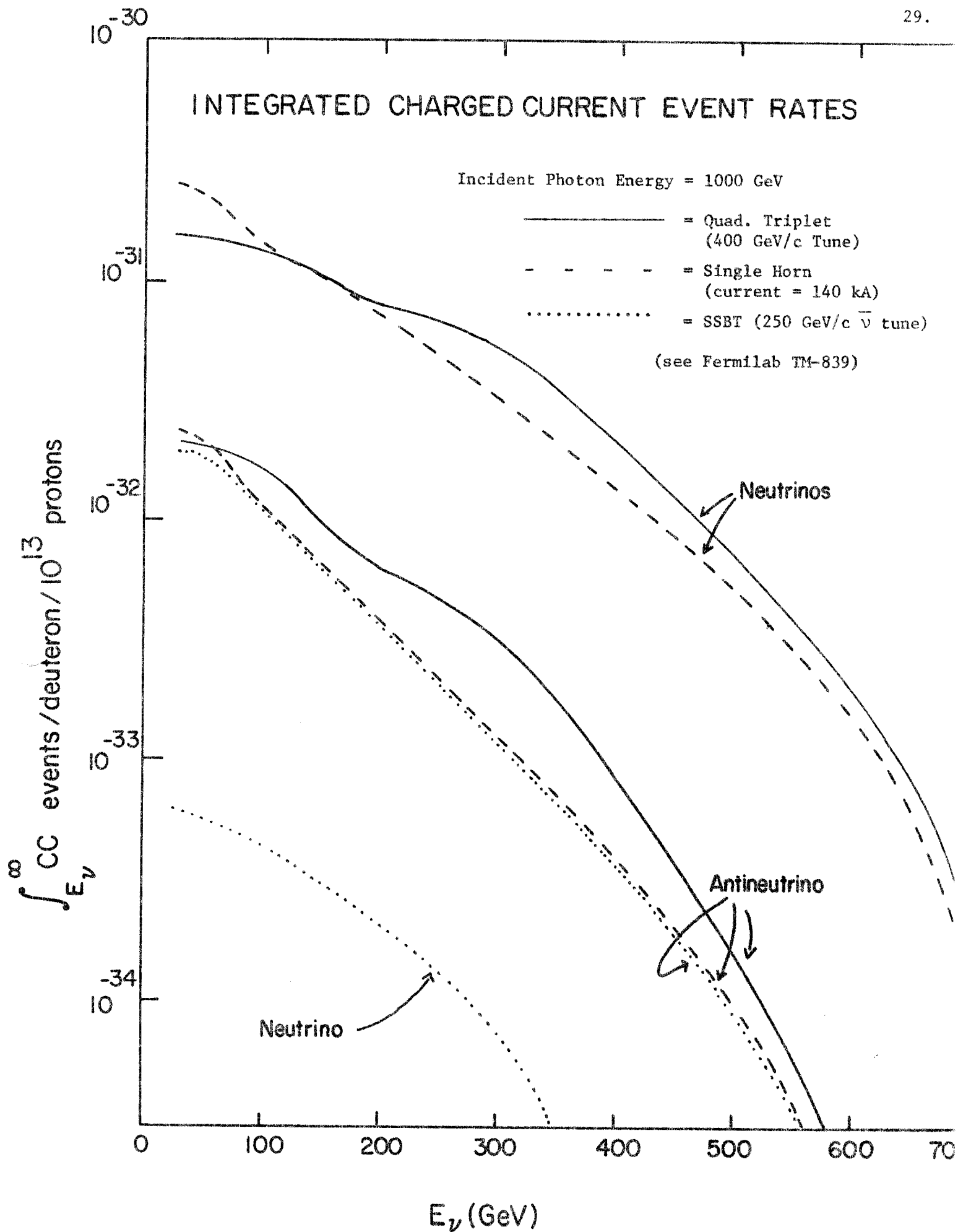


Figure 1.

## QUADRUPOLE TRIPLET BEAM

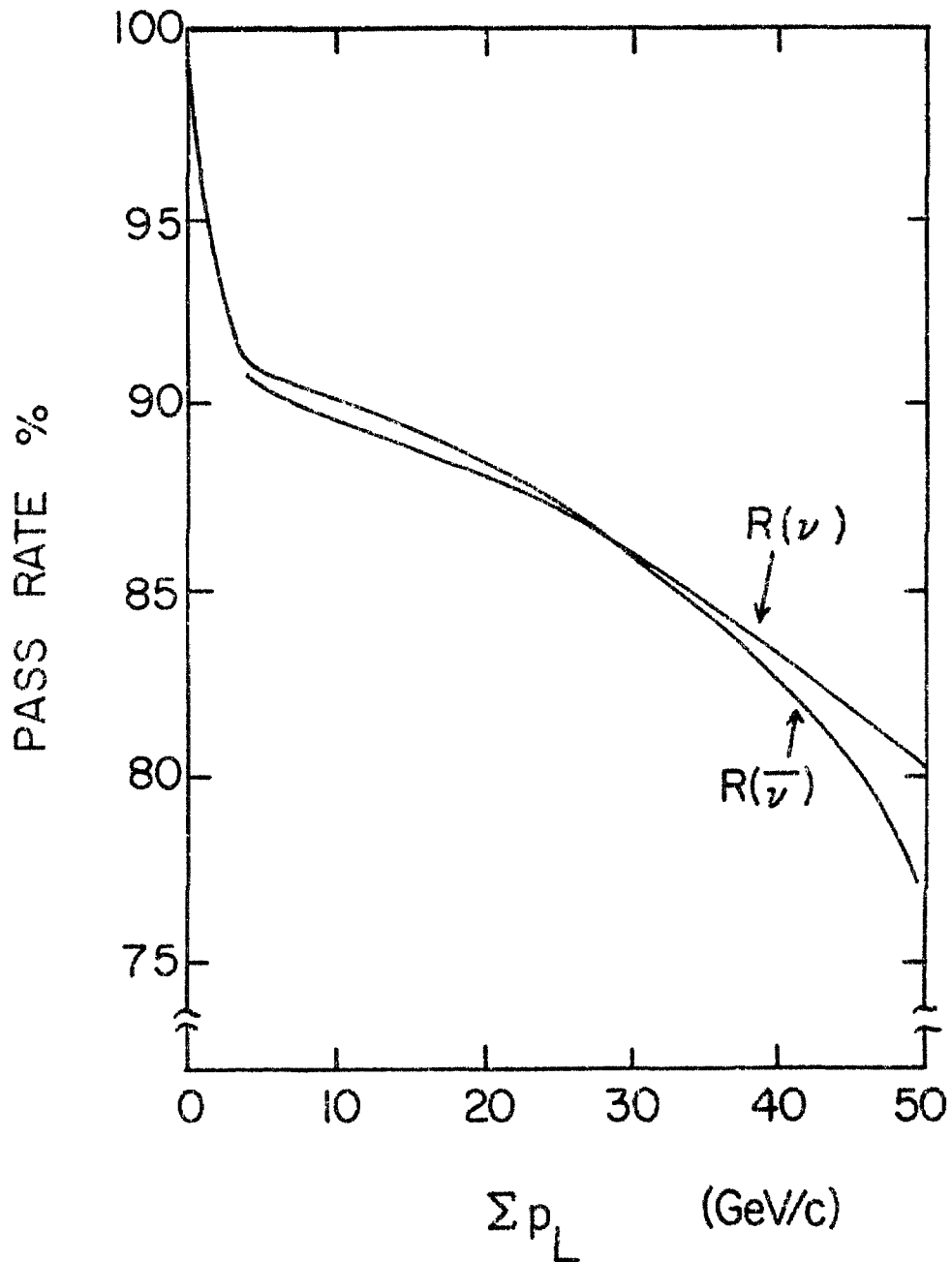
 $E_{inc} = 1000 \text{ GeV/c}$     Tune = 400 GeV/c

Figure 2.

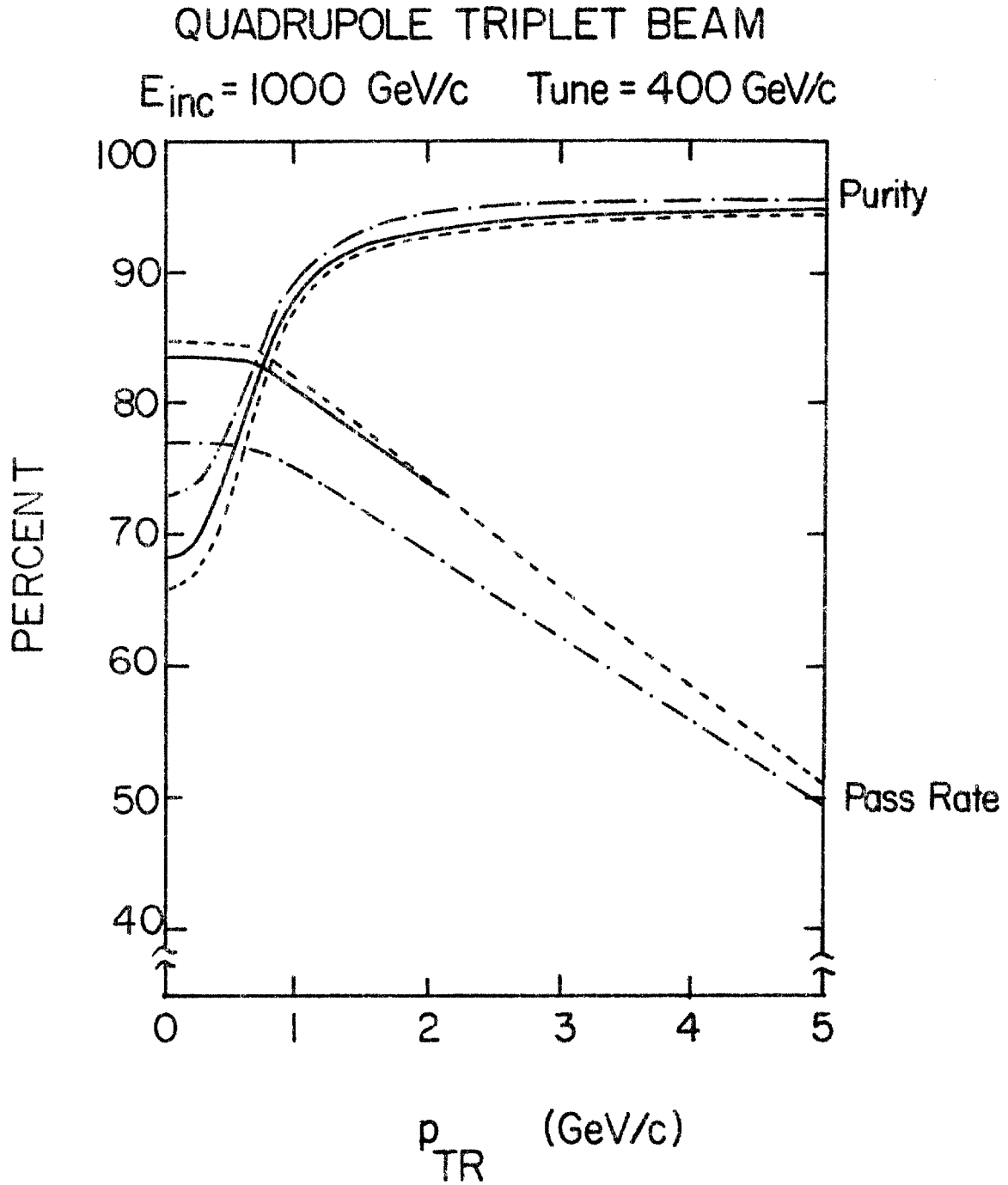


Figure 3.

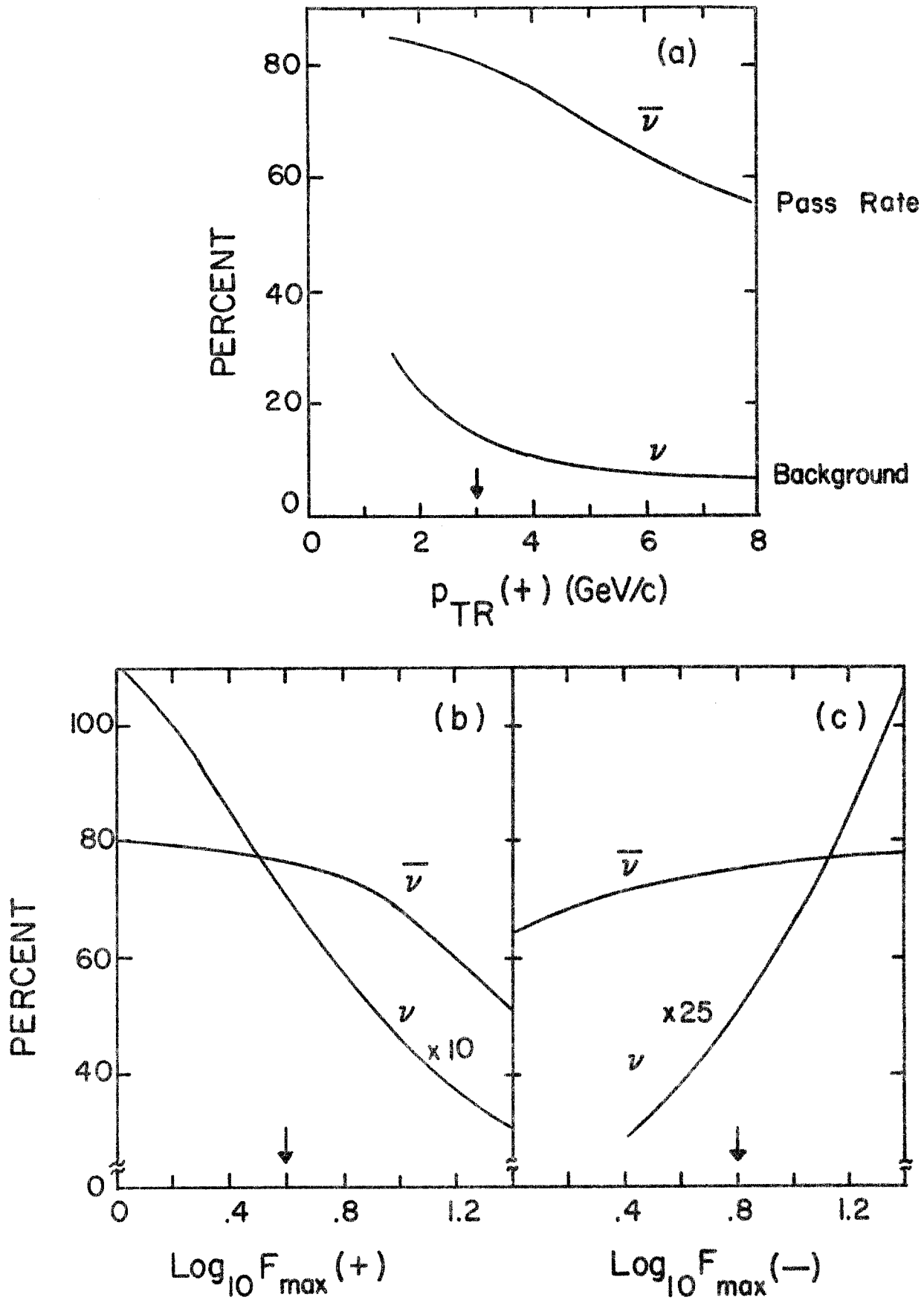


Figure 4.

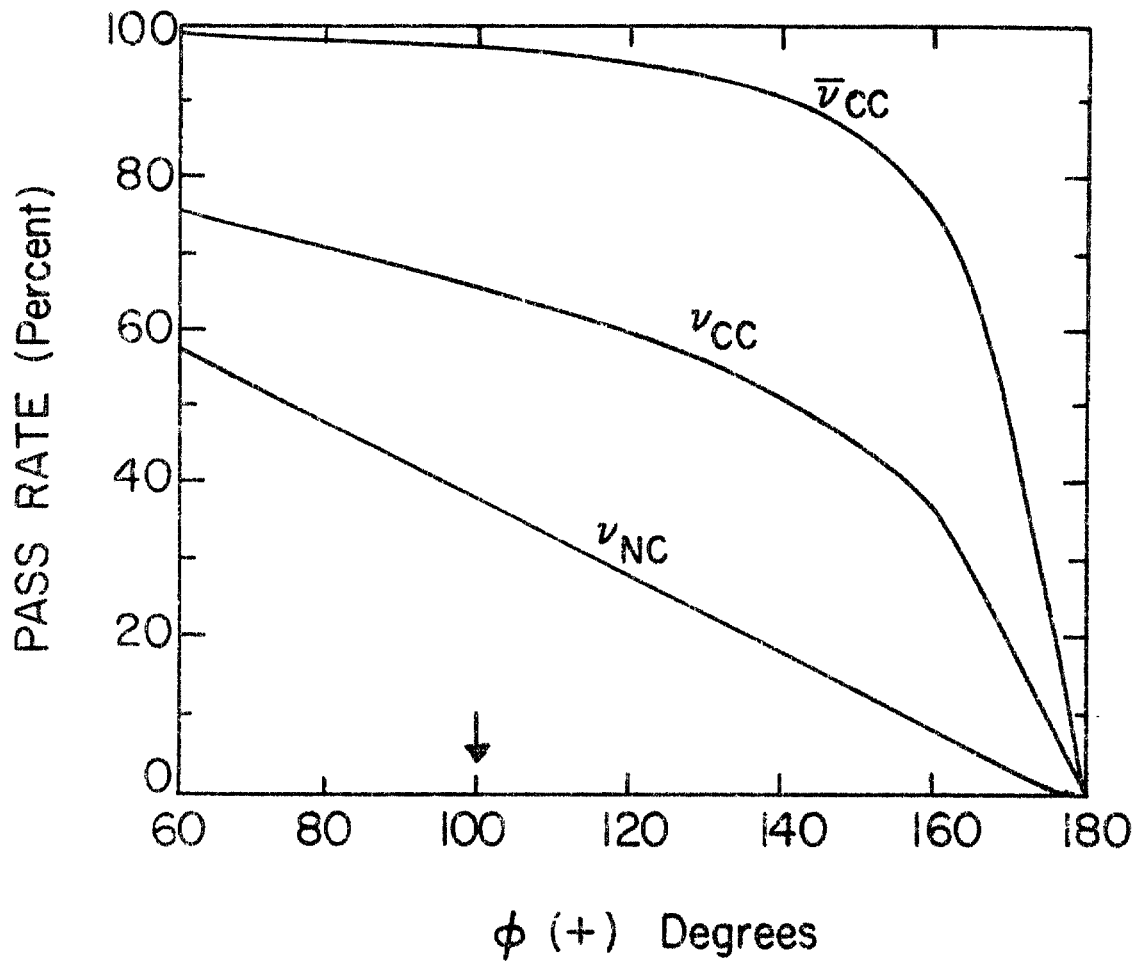


Figure 5.

## APPENDIX A

January 7, 1980

Detection of Neutrino Produced Photons and Electrons by Plates in the 15-ft. Fermilab Bubble Chamber at Tevatron Energies

W.A. Mann and J. Schneps

In 1978 Fermilab approved a test of a downstream plate system inside the 15-foot chamber which was designed for the purpose of detecting photons and electrons from neutrino and antineutrino interactions in hydrogen and deuterium. As it turned out, the plate test was not successful in that the cameras which viewed the regions between plates did not obtain sharp pictures of tracks, and the neutrino-deuterium experiment (E-545) subsequently ran without plates. The antineutrino experiment (E-542) still awaits running time.

According to the Fermilab staff responsible for the plate system (Fig. 1,2), the cure of the problem which led to the difficulty is straightforward. It consists simply in cutting off about ten inches from the top and bottom of the plates so as to eliminate the funneling effect which produced turbulence in the original design. In view of the fact that the plates and their mounting system exist, and that the earlier difficulty can be easily corrected, it becomes evident that reinstallation of the plate system in the chamber may be the simplest and most economical way to achieve good photon and electron detection from neutrino and antineutrino interactions in light liquids. Therefore, it behooves us to examine whether the arguments which would have made the plate system a useful adjunct to the 15-foot chamber at present Fermilab energies still hold true at Tevatron energies, and to compare the plate system to other methods proposed for this purpose.

The advantages of hydrogen or deuterium fills in comparison with heavy liquid fills are the better resolution, the ability to fit exclusive channels,

and the reduction of smearing due to Fermi motion and secondary scatters within a heavy nucleus. The disadvantages are in the event rate and the lack of ability to detect photons and electrons in any great number. The plate system can go a long way toward remedying the latter.

We also point out that the use of the plate system reduces the useable fiducial volume of the chamber from  $18\text{m}^3$  to about  $12\text{m}^3$ , but this is still considerably greater than the  $3\text{m}^3$  available in the BEBC TST.

We will not review in detail the physics advantages that derive except to point out the following:

1. All information on charmed baryon production in neutrino interactions in bubble chambers comes from the analysis of exclusive channels. With the ability to detect  $\Upsilon^0$ 's the number of exclusive charm channels which may be fit may increase substantially. Although much of the charm spectroscopy will be established by the time the Tevatron is available, charm production as a function of neutrino energy and other variables will be of interest.
2. A determination of neutrino energy and the variables  $x$  and  $y$  depends on a knowledge of the energy and momentum of the neutral particles produced in the interaction. At present a statistical correction is used which results in distributions being smeared. Knowledge of neutral particle momenta will sharpen these distributions.

3. A knowledge of neutral particle energy also makes it possible to achieve a better separation of neutral current interactions and will result in a considerable improvement in neutral current distributions.
4. The hadronization of quarks, particularly of the charmed quarks, is aptly studied in neutrino interactions in light liquids. A proper study should take into account hadronization into neutral as well as charged particles.
5. The reaction  $\nu_{\mu} N \rightarrow \mu^{-}$  can be used in deuterium for flux normalization. The plates, used as a  $\gamma$ -ray veto, can rule out background.
6. Using the EMI as a muon detector and the plates as an electron detector, multilepton events in  $H_2$  or  $D_2$  may also be studied.

In 1978 we presented Monte Carlo results on photon and electron detection efficiencies of the "trimmed" plate system for the single horn wide band beam produced by 350 GeV/c protons. For exclusive channel photon production containing  $\pi^0$ 's, we used as input real events of the type  $\nu_{\mu} p \rightarrow \mu^{-} p \pi^{+}$  and  $\nu_{\mu} p \rightarrow \mu^{-} p + N\pi^0$ 's,  $N = 2-6$ , treating the charged pions as  $\pi^0$ 's. For inclusive charged current processes we used  $\gamma$ 's observed in heavy neon-hydrogen. Simulation of  $e^{\pm}$  production was done using published distributions from the reaction  $\nu_{\mu} N \rightarrow \mu^{-} e^{\pm} \chi$ . Probabilities for observing  $\gamma$  and  $e^{\pm}$  induced showers in the 13mm steel plates were estimated from shower tables for copper and probabilities for  $\gamma$  conversion in liquid deuterium were determined from hydrogen data.

We have now extended the calculations to neutrino beams produced by protons of 800 and 1000 GeV/c, using the neutrino energy spectra given by H. Mori. The results are shown in the accompanying figures. Figures 3 and 4 show the momentum and production angle distributions for

photons from the exclusive final state  $\mu^- p^+ \pi^0$ ". Figure 5 shows the number of plates along the line of flight of photons from this final state. Figures 6, 7 and 8 give the same information for inclusive photons from the final states  $\mu^- \nu^0 \chi + \gamma$ 's. Figure 9 shows photon detection efficiencies as a function of  $E_{\text{vis}}$  for both categories of events, and Figure 10 shows this as a function of final state photon multiplicity. Finally, Figure 11 shows the capability of the plates for vetoing final states containing  $\pi^0$ 's.

At 350 GeV/c we conclude that the detection efficiency is 72% of  $\gamma$ 's from inclusive processes and 36% of  $\gamma$ 's from the one  $\pi^0$  channel. The 72% detection efficiency would make it possible to reduce the undetected hadronic energy in inclusive processes to the 10% level. The system's utility for separating fittable exclusive channels is seen from Fig. 11. It is  $\geq$  85% effective as a shield against final states with 2 or more  $\pi^0$ 's. In the case of single  $\pi^0$  final states, the system is  $\geq$  70% effective if one or more charged pions is produced along with the  $\pi^0$ . Only for events where the only pion produced is the single  $\pi^0$  does the efficiency drop below 50%. At 800 and 1000 GeV/c, as the figures show, the conclusions are almost identical, there being only a slight increase in detection efficiencies.

Up to this point we have emphasized the improvement in the determination of total neutral energy and momentum and in the use of the plates as a  $\pi^0$  veto. It may also be possible to make some use of the plate information to reconstruct  $\pi^0$ 's and use them in exclusive channel fits. Using the predicted uncertainty of  $\sim 30\%$  in  $\gamma$  energies, the Purdue group, in a Monte Carlo simulation, found a  $\pi^0$  mass peak with FWHM of  $\sim 80$  MeV. Use of the kinematics of the production vertex will improve this.

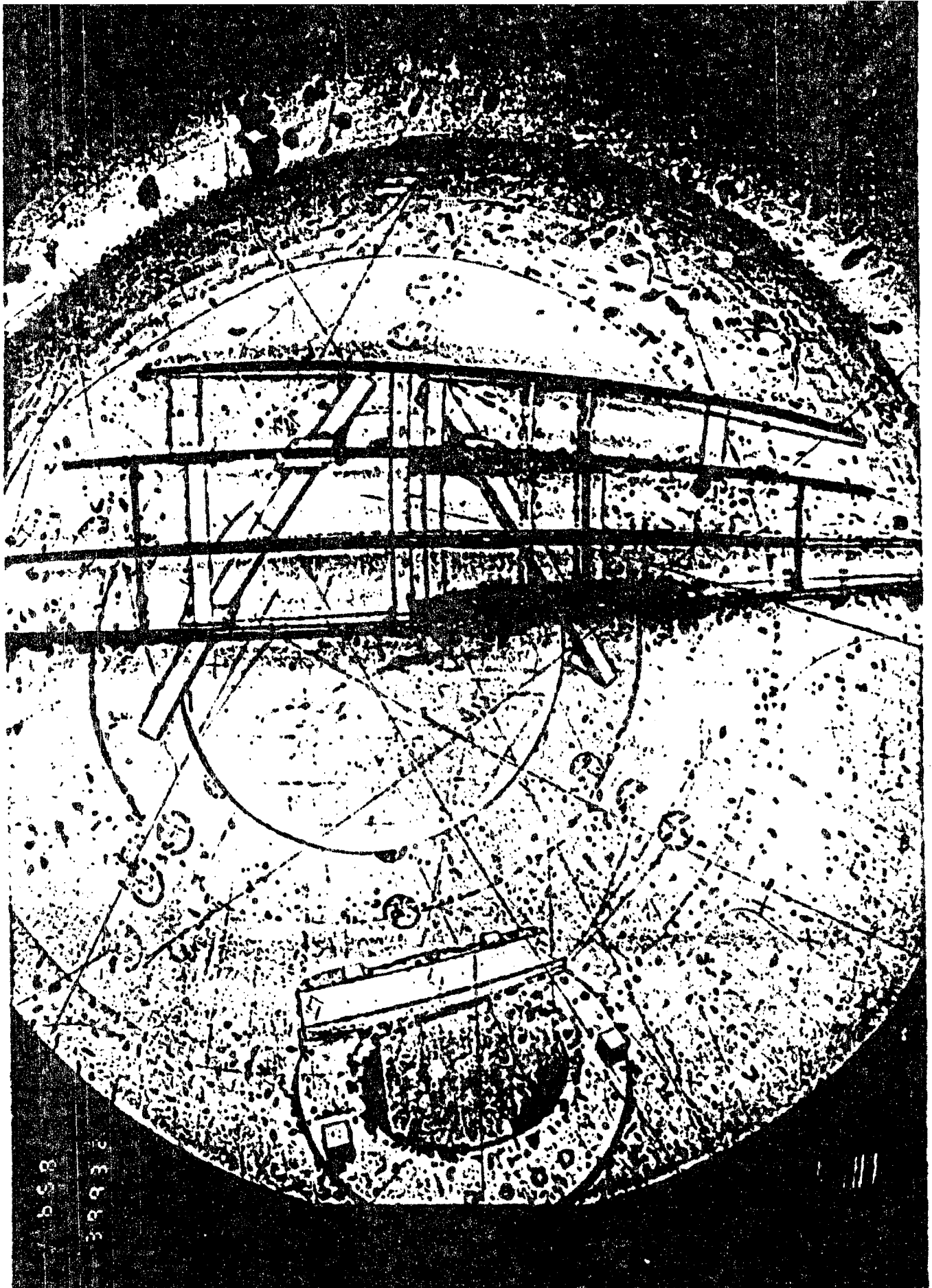
The efficiency for finding  $e^+$  from the final state  $\mu^- e^+ \chi$  was found to be  $\sim 73\%$ . It is then necessary to know what kind of background to  $e^+$  events could be caused by  $\pi^+$  incident on the plates. The BC-65 experiment at SLAC, using three tantalum plates of 1.0 radiation length, showed that at 1.6 GeV/c only one  $\pi^+$  in 20,000 caused a fake  $e^+$  shower and at 3.1 GeV/c only one in 100,000 did so, whereas true  $e^+$  tracks caused a good signature  $(94 \pm 1)\%$  of the time. The Japanese group at Tohoku, using two tantalum plates each of 1.6 radiation lengths, found one in 10,000  $\pi^+$  simulated an  $e^+$  shower. The pions came from  $\pi^+ p$  interactions at 8 GeV/c and the result is consistent with the SLAC data. Based on this data it is estimated that in the proposed 15-foot plate system one  $\pi^+$  in 7000 will fake an  $e^+$  at 1.6 GeV/c and one in 30,000 will do so at 3.1 GeV/c, while  $\sim 95\%$  of true  $e^+$  will be identified.

A downstream plate array poses new possibilities and also some problems for identifications and measurement of charged hadrons and muons in neutrino events. It has been pointed out that energetic protons which interact upstream of the plates would, on the average, yield less energetic electromagnetic showers in the plates than would secondary interactions of  $\pi^+$  mesons, hence the plates would enable some discrimination.<sup>(1)</sup> The probability that a hadron of several GeV/c momentum undergoes a hadronic interaction in traversing a plate is  $\sim 7\%$ . For negative tracks, this additional scattering within the visible chamber volume provides discrimination between final state  $\pi^-$ 's and  $\mu^-$ 's. On the other hand, multiple scattering in the plates and reduction of measurable track length due to strong interactions in the plates will result in reduced momentum resolution for charged tracks. In the available fiducial volume upstream of the plate array, all primary vertices and secondary  $V^0$  vertices are measured in liquid deuterium where track reconstruction is optimal.

Furthermore, track lengths greater than a meter will be typical. However, improved charged track resolution could be achieved by measuring tracks through the plates. The motivation for doing this is indicated by Figure 12, which shows that, in existing FNAL wide-band exposures, track momenta for charged hadrons and muons are typically 0-20 GeV/c (Figs. 12a, b)<sup>(2)</sup> for which track lengths of 1-2 meters are ideal (Fig. 12c)<sup>(3)</sup>. In neutrino reactions at the Tevatron the muon momentum spectrum will shift upward by tens of GeV/c. In order to avoid substantial deterioration of momentum resolution and in order to associate muon tracks with EMI hits, candidate muon tracks will certainly need to be reconstructed through the plate array; moreover, reconstruction of all charged tracks through the plates should probably be attempted.

## FOOTNOTES AND REFERENCES

1. FNAL Proposal E-542, "Proposal for an Extension of E(31)/(390) to Study  $\bar{\nu}_p/\bar{\nu}_n$  Interactions in the 15-Foot Bubble Chamber with  $\gamma$ -Converting Plates", Spokesman: A.F. Garfinkel.
2. Data from  $\nu_\mu \cdot N$  Exposures: Fig. 12a. IIT, Maryland, Stony Brook, Tohoku, Tufts Collaboration (E-545). Fig. 12b. Columbia-BNL Collaboration, Thesis by E.E. Schmidt, Jr.
3. Fig. 12c from J. Lach, "Strong Interaction Physics in the NAL Bubble Chamber", in Proceedings of International Conference on Bubble Chamber Technology, Vol. I, p.42, June 1970.



553

33936

FIGURE A.1

# FIGURE A.2

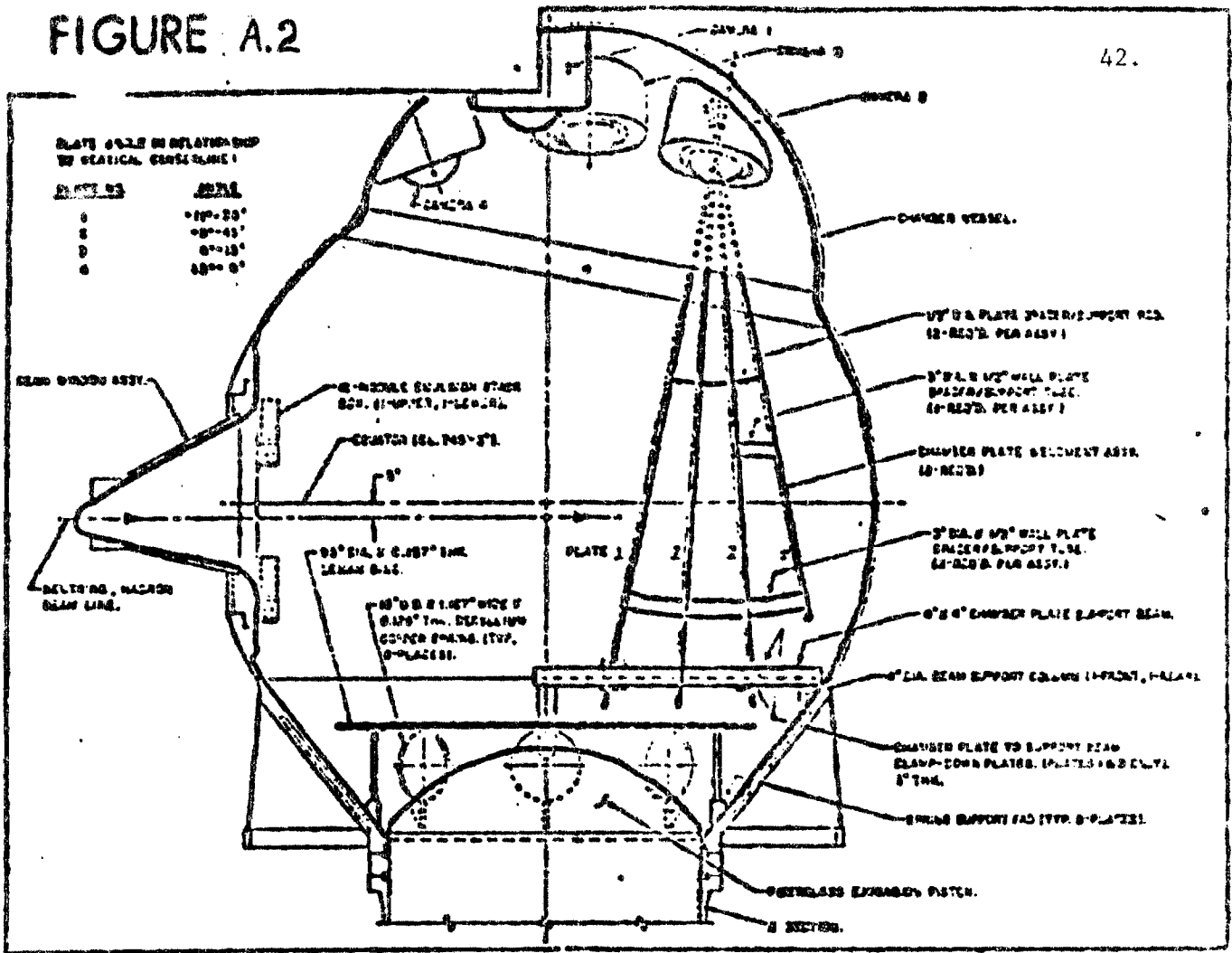


PLATE SIZES IN RELATIONSHIP  
TO STATICAL CONSIDERATIONS

PLATE NO.	ANGLE
1	15°-25°
2	25°-45°
3	45°-65°
4	65°-90°

HEAD BRIDGE ASST.

BEARING, WAGON  
BEAM LINE.

4\"/>

CONCRETE 12\"/>

1\"/>

1\"/>

PLATE 1

2

2

2

2

CHAMBER VESSEL.

1/2\"/>

1/2\"/>

CHAMBER PLATE ELEMENT AREA  
12\"/>

1/2\"/>

6\"/>

1\"/>

CHAMBER PLATE TO SUPPORT BEAM  
CLAMP-DOWN PLATES (SPACED 1\"/>

BRIDGE SUPPORT (AD. 1\"/>

GLASS EXTENSION PATCH.

A SECTION.

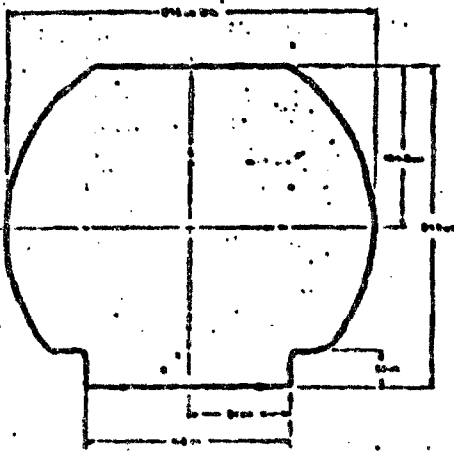


PLATE 1

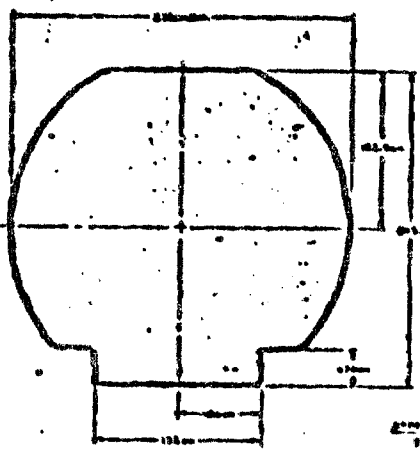


PLATE 2

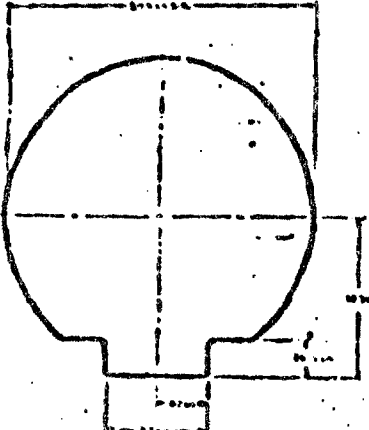


PLATE 3

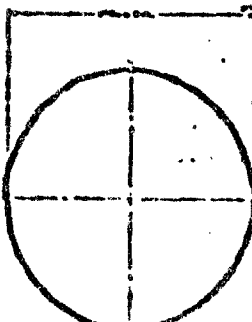


PLATE 4

REMARKS:  
PLATE 1 - 1/2\"/>

NOTES:  
1) ALL PLATES 1/2\"/>

2) ALL PLATES 1\"/>

Fig. A.3

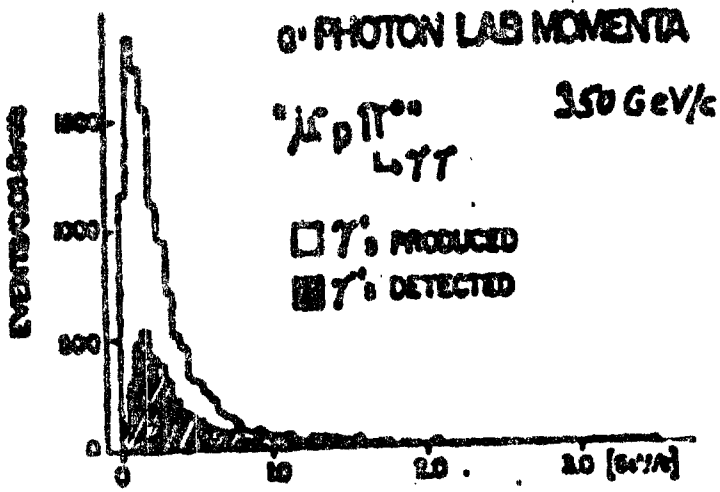


Fig. A.4

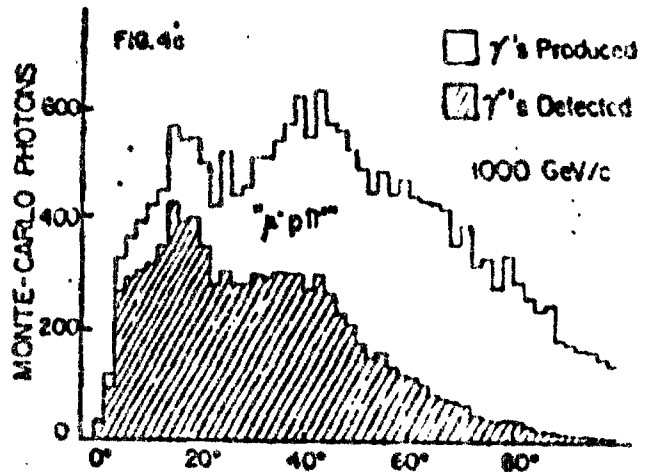
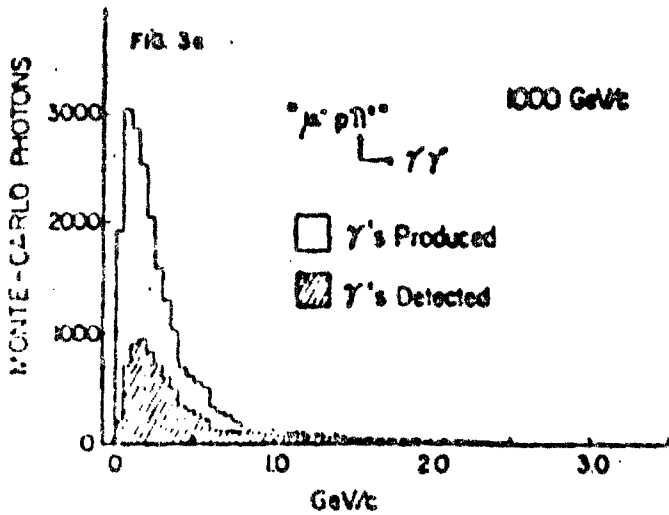
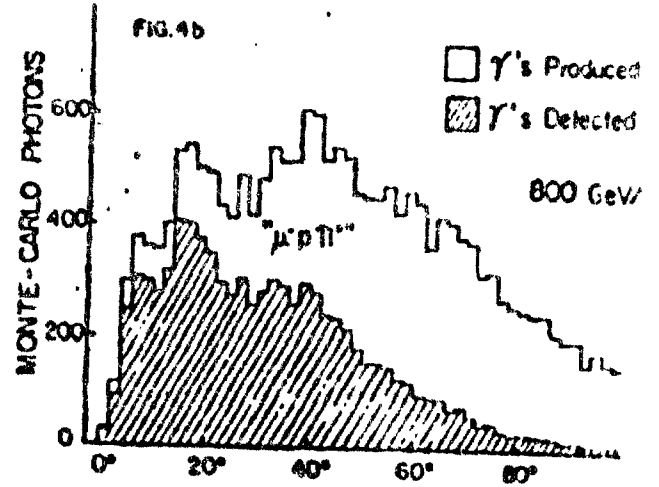
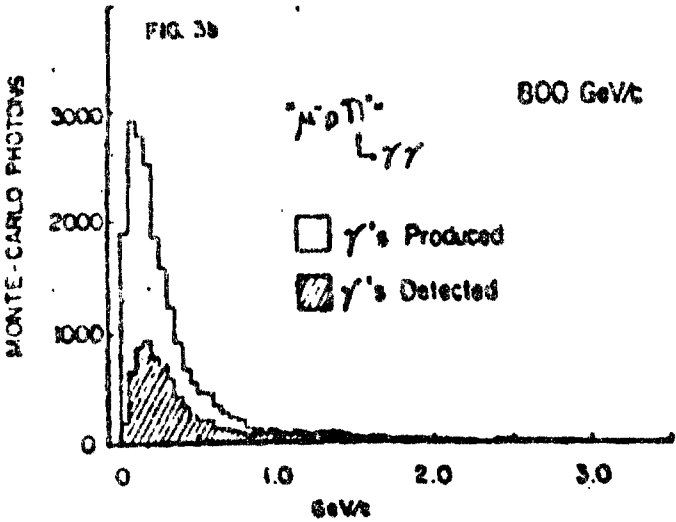
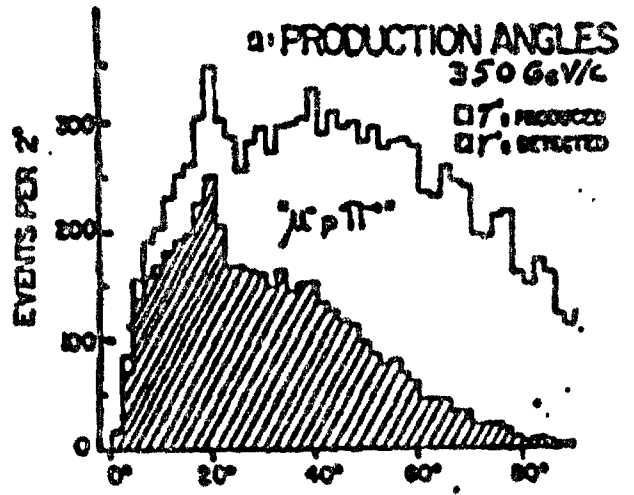


Fig. A.5

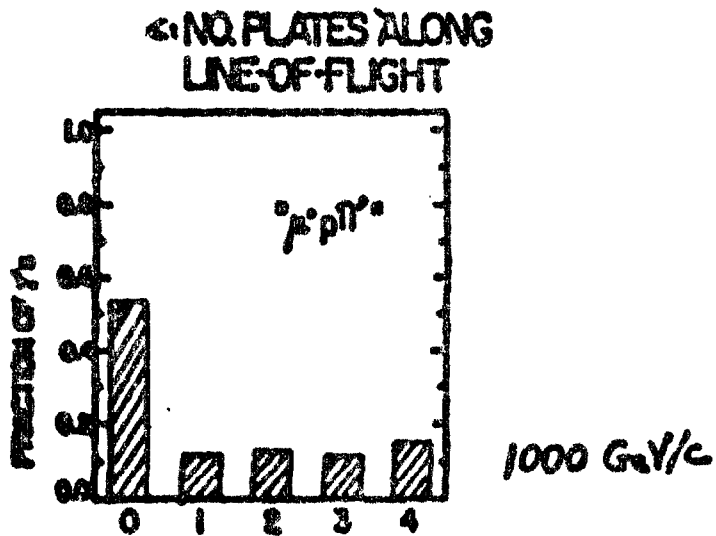
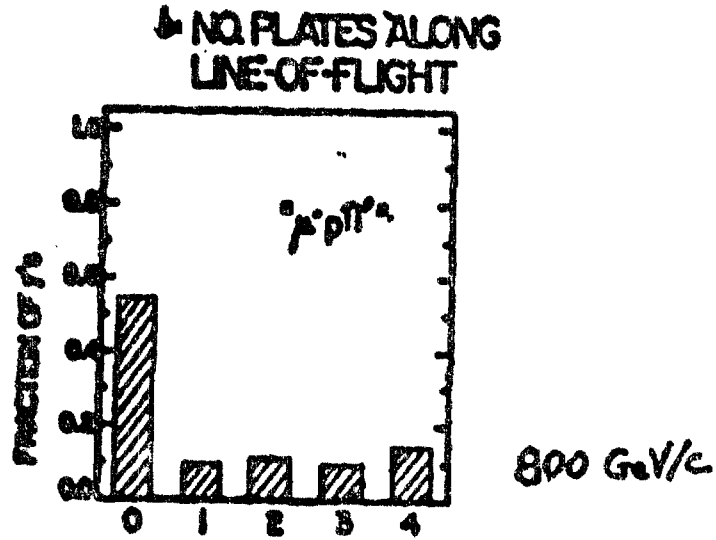
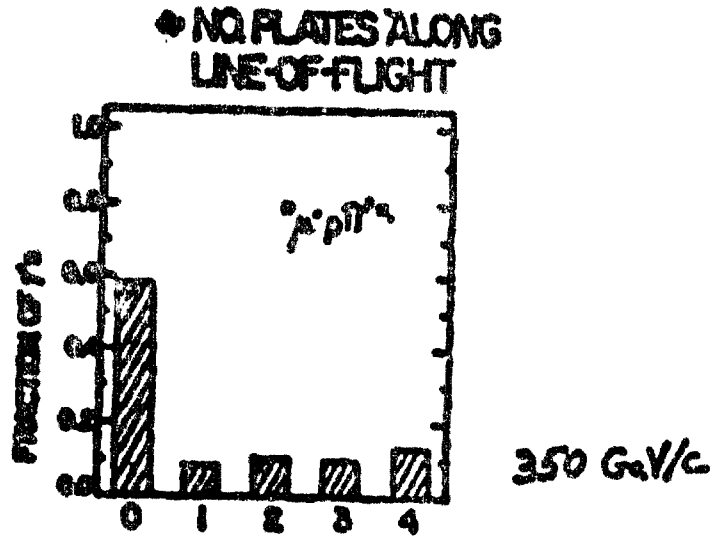


Fig. A. 6  
a) PHOTON LAB MOMENTA

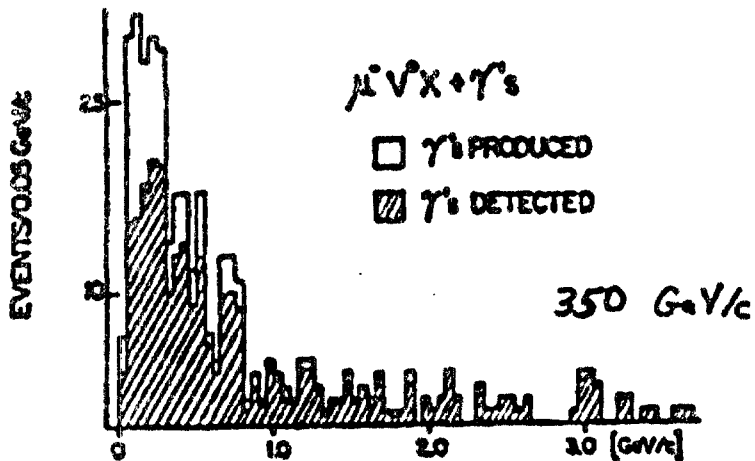


Fig. A. 7  
a) PRODUCTION ANGLES

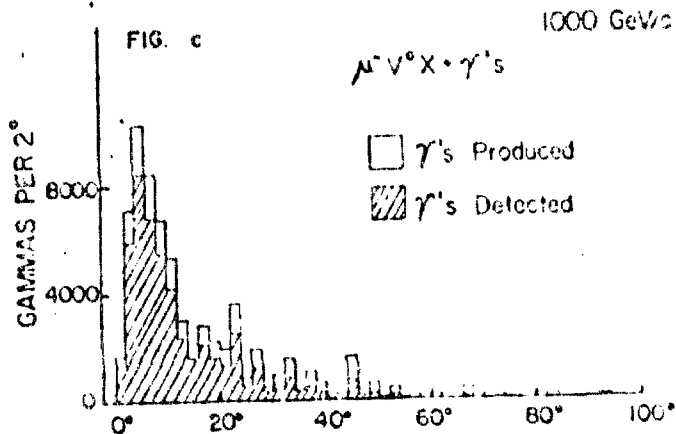
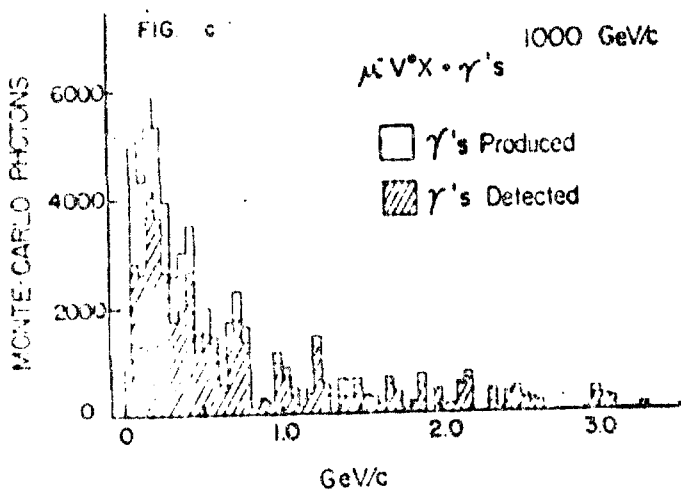
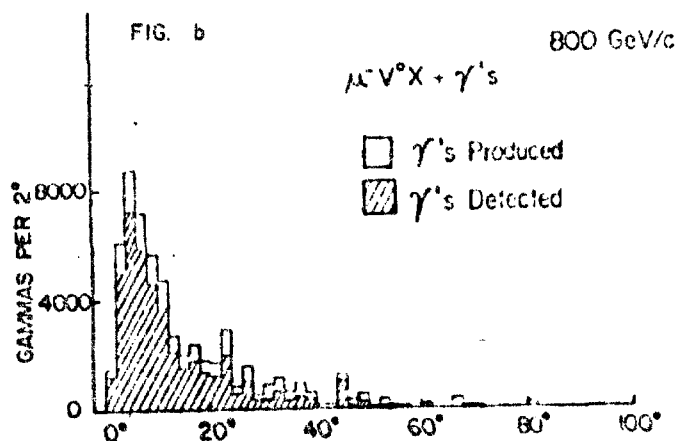
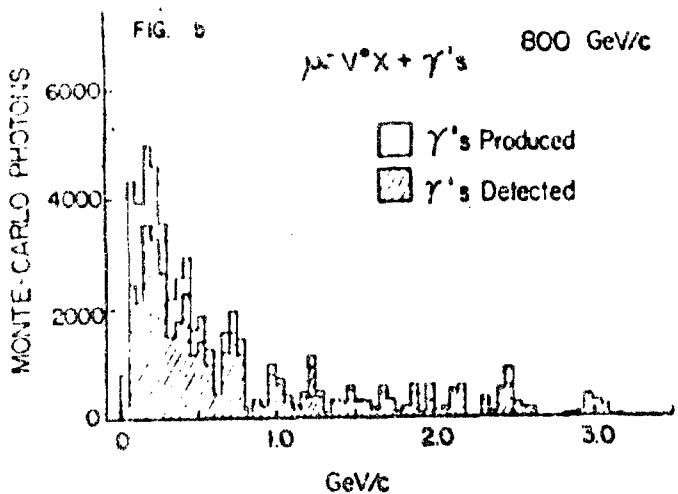
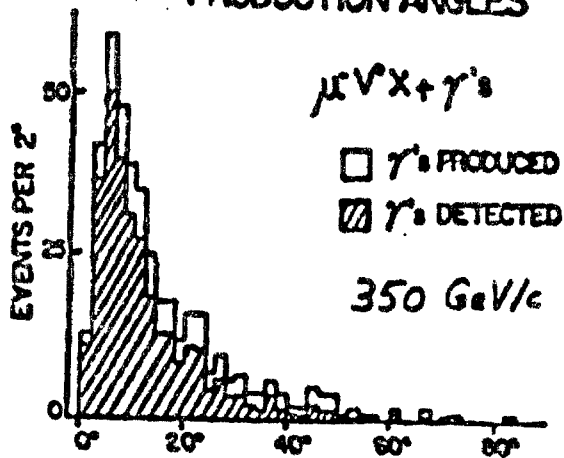
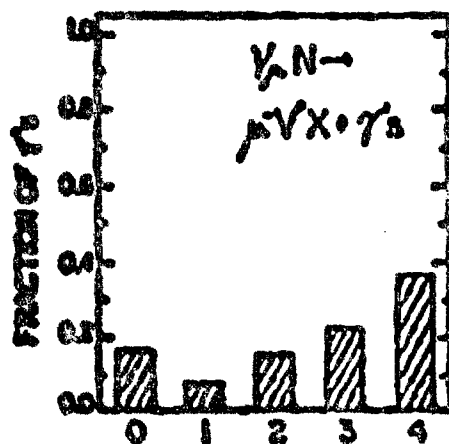


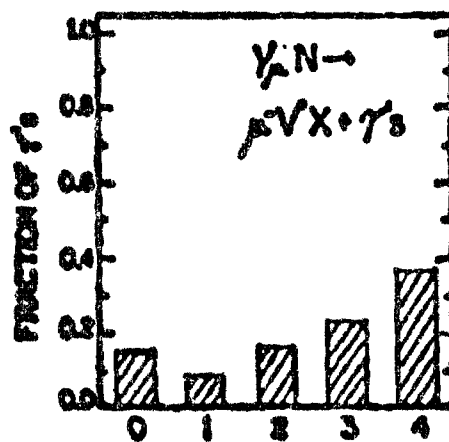
Fig. A. 8

a. NO. PLATES ALONG  
LINE-OF-FLIGHT



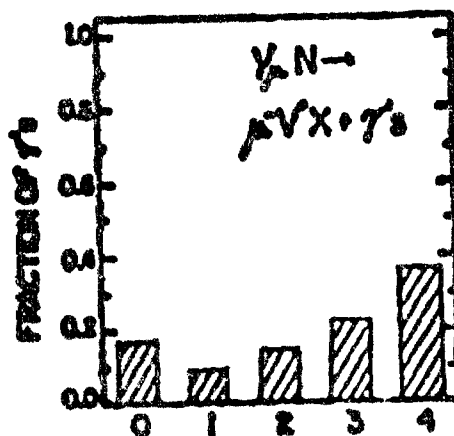
350 GeV/c

b. NO. PLATES ALONG  
LINE-OF-FLIGHT



800 GeV/c

c. NO. PLATES ALONG  
LINE-OF-FLIGHT



1000 GeV/c

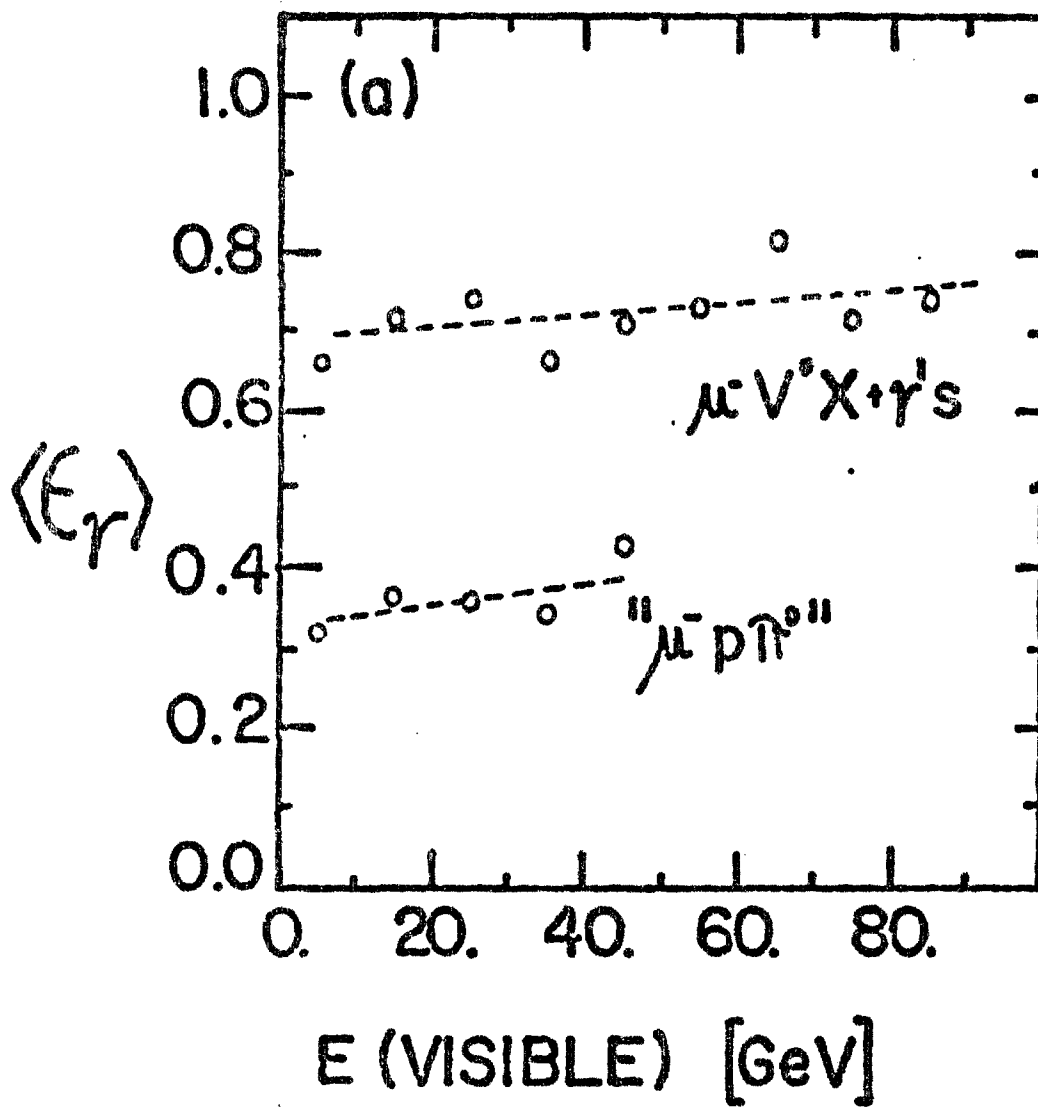


FIGURE A.9

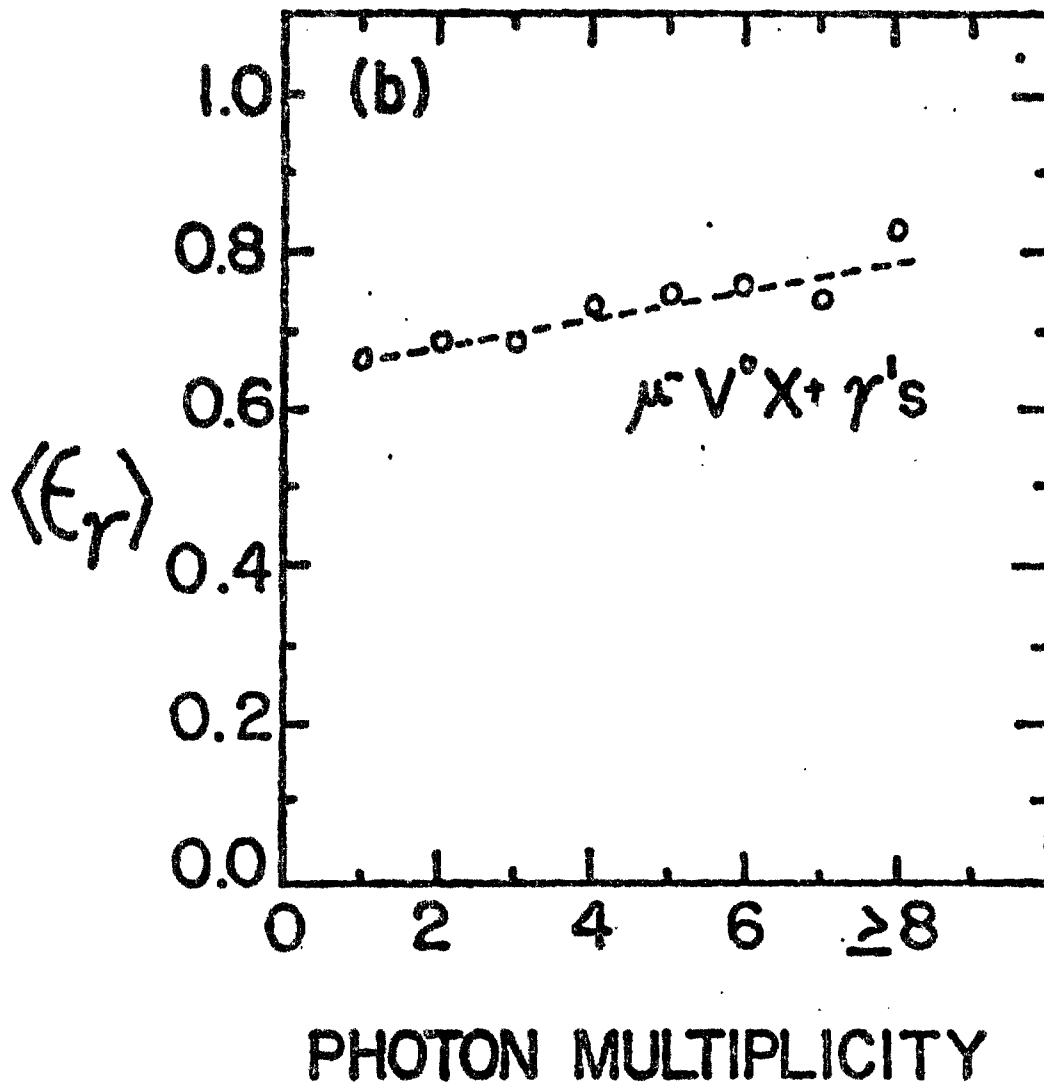
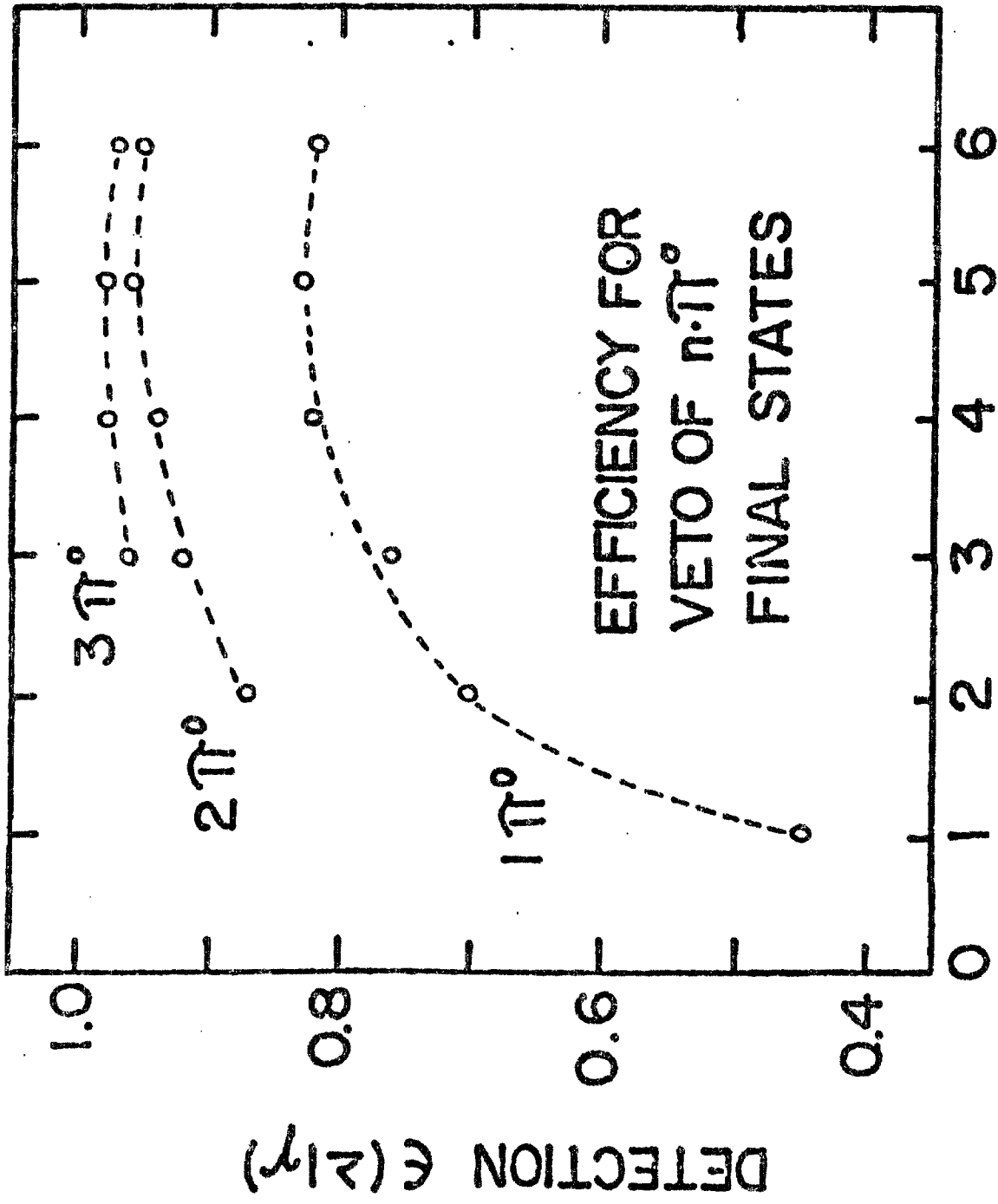


FIGURE A.10



TOTAL PION MULTIPLICITY

FIGURE A.11

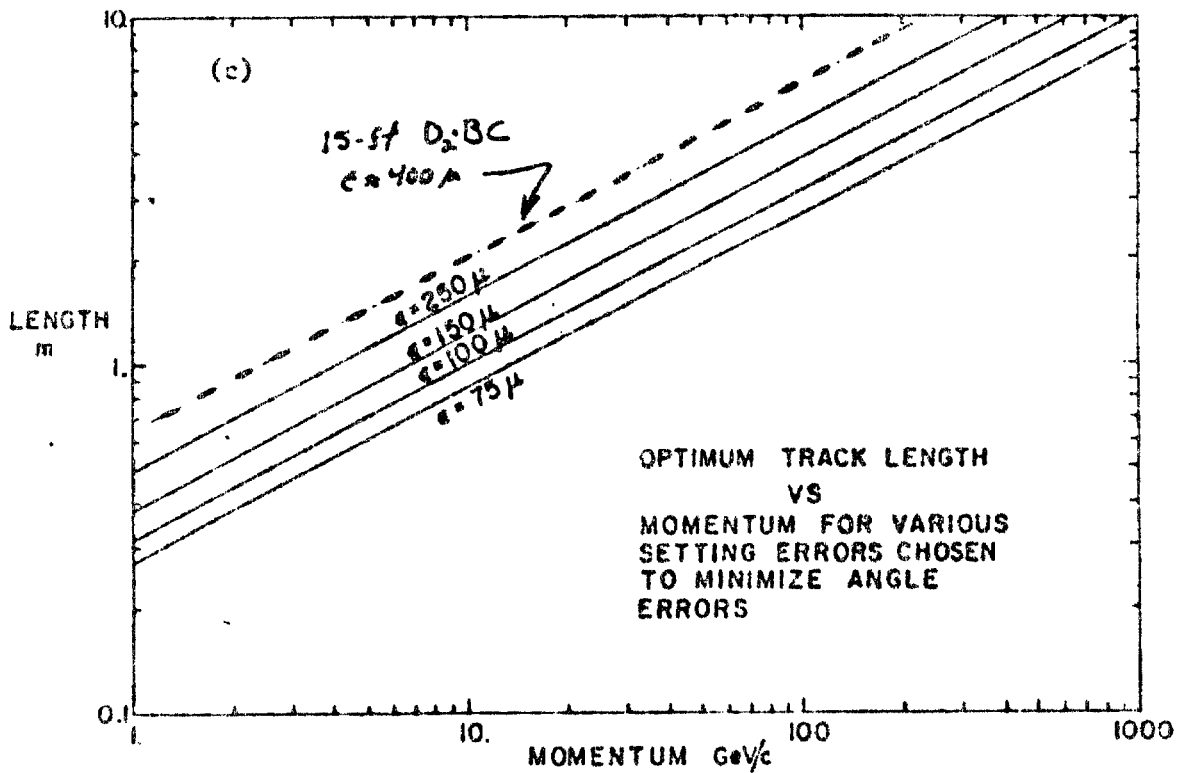
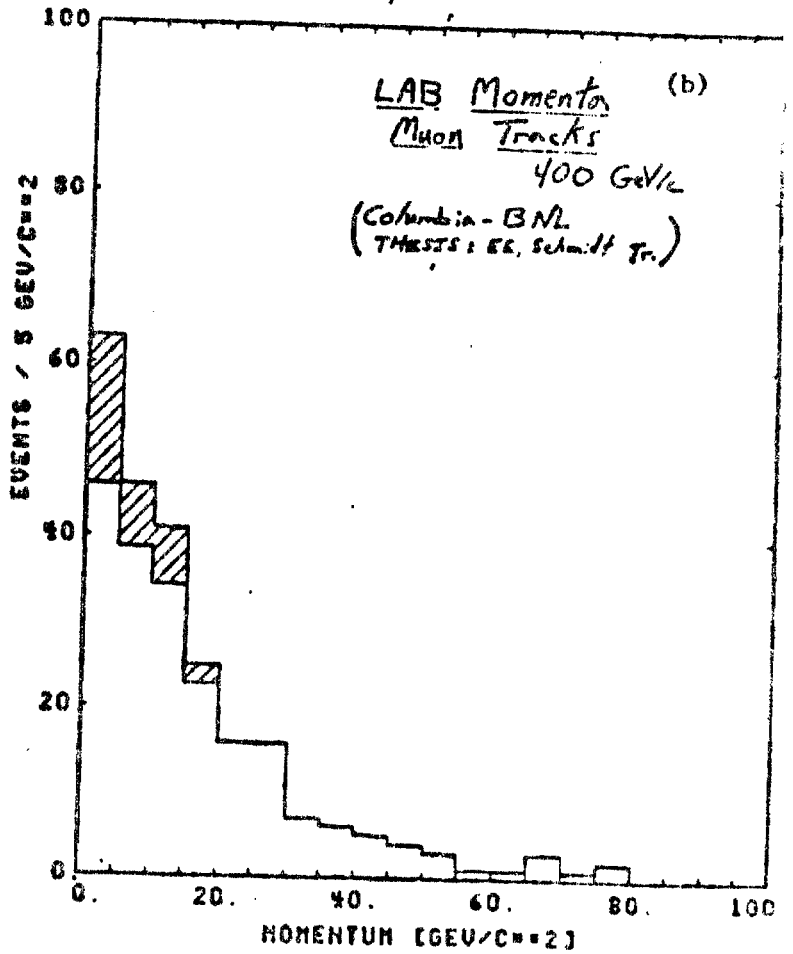
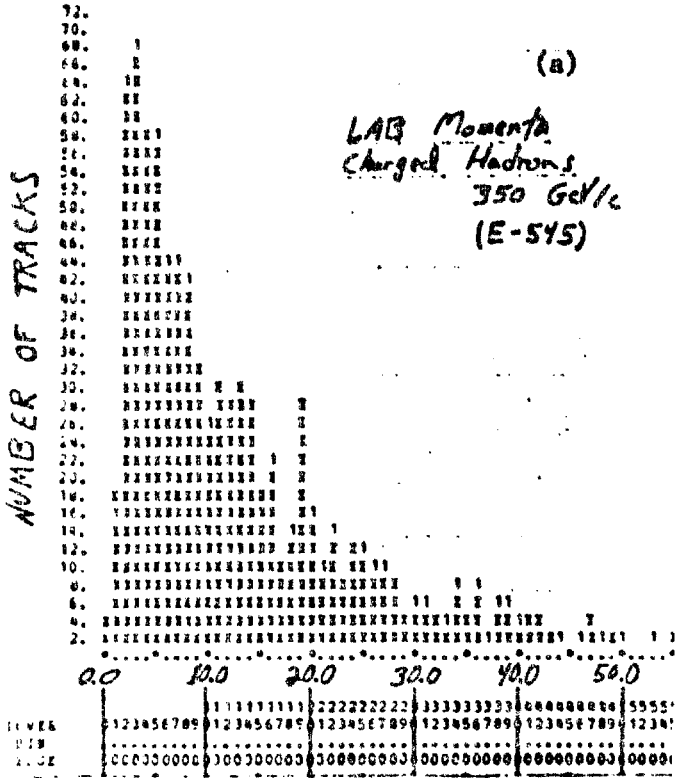


Figure A.12

## APPENDIX B

## SUMMARY OF PROGRESS IN E-545

As stated in the introduction, at the time of writing about 2/3 of the film has been completely processed and all the events found are now on a DST. The other 1/3 of the film has been double-scanned and the events found are now being measured and passed through our geometric and kinematic analysis programs. This work will be finished in September 1980 at which time a full and complete DST for this experiment will exist. The total time elapsed from the run at Fermilab to the complete DST will be about 20 months.

At the same time, we have been pursuing the physics analysis of various topics. Reports on progress from E-545 have been presented at the April 1979 Washington A.P.S. Meeting, at the International Conference Neutrino 79 which took place at Bergen in June 1979, at the International Photon-Lepton Conference at Fermilab in August 1979, at Japanese Physical Society meetings in October 1979 and March, 1980, and at the January 1980 Chicago APS meetings. Further reports will be presented at the 1980 Washington meetings and at international conferences to be held in the summer of 1980, notably the International High Energy Physics Conference in July at Madison. In addition, two papers are now ready to be submitted to letter journals and others are in preparation.

In this section, we briefly report on the present status of our physics analysis with the expectation that more substantial physics results will be available in the near future.

- (1) Charged Current Reactions - the n/p ratio and a comparison of the quark distributions  $d_n(x)$  and  $d_p(x)$

We have determined the value of the ratio  $R = \sigma(\nu n \rightarrow \mu^- X) / \sigma(\nu p \rightarrow \mu^- X)$

from our data. The separation of  $\nu d$  interactions into neutron target and proton target events is complicated by the phenomenon of rescattering, in which the products of an interaction with one of the nucleons in the deuteron interact with the other nucleon. The correction for rescattering is important because its effect on  $\nu n$  collisions is to change the topology of an event to that of a  $\nu p$  interaction, while the topology of a  $\nu p$  event in which rescattering occurs remains unchanged. The fraction of  $\nu d$  events which rescatter has been estimated to be  $0.094 \pm 0.035$  in a phenomenological study by extrapolating the rescatter rates observed in  $p d$  and  $\pi d$  interactions to  $\nu d$  collisions. This is done by assuming the rescatter rate is a linear function of cross section.

With the present accumulation of data, we find the value of the ratio  $R$  to be  $R = 1.83 \pm 0.15$ . About 1/3 of the error is statistical and 2/3 is due to the uncertainty in the fraction of events which contain rescatters in the deuteron.

In addition we have for the first time, by studying  $\nu n$  scattering, compared the structure functions  $d_n(x)$  and  $d_p(x)$  for the valence down quark in neutron and proton respectively. The general feature of these distributions (see Fig.B1) is that  $d_n(x)$  is considerably broader than  $d_p(x)$ . The relative broadness of  $d_n(x)$  compared to  $d_p(x)$  is consistent with the charge symmetric SU(6) breaking effect seen by SLAC when comparing  $e p$  with  $e n$  deep inelastic reactions. (1) Detailed study of the structure functions as a function of  $Q^2$ , now in progress, can reflect both QCD and higher twist (primary diquark) effects. In addition, the study of non-singlet cross sections obtained from the difference  $\frac{d\sigma}{dx}(\nu n) - \frac{d\sigma}{dx}(\nu p)$ , (see Fig.B2, the Feynman-Field fit to our preliminary data), while primarily useful for the study of valence quark properties, can also be used in the small  $x$  region to search for asymmetries between  $u\bar{u}$  and  $d\bar{d}$  in the sea.

The quantity  $3[F_1(ep) - F_1(en)] - [F_1(\nu n) - F_1(\nu p)] = 2(\bar{u} - \bar{d})$  is a direct measure of such an asymmetry, which is already suggested from a study of ep and en interactions alone. (2)

Finally, in this neutrino run, we were able, by using the two-plane EMI, to identify  $\bar{\nu}_\mu$  interactions, and determine their n/p ratio to be  $0.56 \pm 0.16$ .

To obtain information about individual structure functions we can normalize our neutrino flux to our observed number of  $\nu - d$  ( $I = 0$ ) events, using the measured value of  $\sigma_{TOT}^{CC}(I = 0)$ . We have checked that the flux determined by quasi-elastic events agrees with this method to the statistical accuracy ( $\sim 20\%$ ) allowed. We shall compare our  $y$  distributions with detailed Monte Carlo calculations in order to determine the relative coefficients of terms proportional to  $1$  and  $(1 - y)^2$ . Eventually, we will also be able to combine our  $\nu d$  data with  $\bar{\nu} d$  data from the BEBC collaboration at CERN.

## (2) The Callan-Gross Relation

We have tested the Callan-Gross relation,  $F_2(x) = 2xF_1(x)$  in deuterium. The quantity  $R = 1 - \frac{f_1}{f_2}$ , where  $f_1 = \int_0^1 2xF_1(x)dx$  and  $f_2 = \int_0^1 F_2(x)dx$ , is given in Table I for this experiment as well as for others. We note that the result in deuterium is considerably better than in bubble chamber experiments using heavier liquids and comparable with the CDHS counter experiments. In addition, the use of a deuterium target allows us to test the relation separately for neutrons and protons.

Table I  
Test of Callan-Gross Relation

	N(n+p)	n	p
This exp. E-545 (D <sub>2</sub> )	-0.01 $\pm$ 0.07	0.001 $\pm$ 0.10	-0.03 $\pm$ 0.11
BEBC <sup>(a)</sup>	0.11 $\pm$ 0.20		
GGM <sup>(a)</sup>	0.32 $\pm$ 0.21		
CDHS <sup>(b)</sup>	-0.03 $\pm$ 0.04		
CITFR <sup>(c)</sup>	0.17 $\pm$ 0.09		

(a) P.C. Bosetti et al., Nucl. Phys. B142, 1 (1978).

(b) C.D.H.S. Collaboration, IX Int. Conf. on High Energy Physics, Tokyo (1978).

(c) B.C. Barish et al., ibid.

### (3) Neutral Current Interactions

We have found that it is possible to obtain a rather clean sample of  $\nu_\mu$  neutral current events by choosing those events with  $|p_{\text{TR}}| < 1.0 \text{ GeV}/c$ , where  $p_{\text{TR}}$  is the transverse momentum relative to the remaining charged particles of the negative particle with the highest transverse momentum relative to the incident beam. In this sample, there exist backgrounds due to  $\nu_\mu$  and  $\bar{\nu}_\mu$  charged current interactions where the  $\mu$  is not identified,  $\bar{\nu}_\mu$  neutral current interactions and neutral hadronic induced events. The  $\nu_\mu$  background is corrected for by a Monte Carlo of the  $p_{\text{TR}}^2$  spectrum of  $\mu^-$ ,  $\bar{\nu}_\mu$  background by using the EMI to identify  $\mu^+$ , and  $\bar{\nu}_\mu$  neutral current events by using known results for  $\bar{\nu}_\mu(\text{NC})/\bar{\nu}_\mu(\text{CC})$ . The neutral hadronic

background is essentially eliminated by the cut  $\Sigma p_L > 11 \text{ GeV}/c$ , where  $p_L$  is the longitudinal momentum of an outgoing charged particle with respect to the beam direction.

Using our usual methods for separating n from p events, we obtain the following results for the ratios  $R = \text{NC}/\text{CC}$ :

On deuterium	$R_d = 0.29 \pm 0.04$
On protons	$R_p = 0.47 \pm 0.11$
On neutrons	$R_n = 0.19 \pm 0.05.$

Using the results on n and p, and making appropriate experimental corrections, we are able to extract the neutral current coupling constants  $u_L^2$  and  $d_L^2$ . A preliminary result is shown in Fig.B3.

#### (4) Strange Particle Production

At the present time, about 80% of the  $V^0$  events in our film have been analyzed and we are studying  $V^0$  production in both charged and neutral current events. In charged current events we find the following overall ratios:

$$\frac{\sigma(K^0)}{\sigma(\text{all CC})} = 0.132 \pm 0.05; \quad \frac{\sigma(\Lambda^0)}{\sigma(\text{all CC})} = 0.057 \pm 0.003;$$

and  $\sigma(\bar{\Lambda}^0)/\sigma(\text{all CC}) = 0.002 \pm 0.001$ . The results are about the same on neutrons and protons. More detailed investigations of the properties of these events are underway. Preliminary results show that the x distribution in the valence region is much broader for neutrons than for protons, as is the case for all charged current events. Striking peaks are also seen at small x indicating that a considerable fraction of the  $K^0$  and some of the  $\Lambda^0$  particles are made in interactions of the neutrino with sea quarks, including

$\nu + s \rightarrow c + \mu^-$ . This kind of detailed strange particle production data can complement the global sea quark content information provided by counter experiments. Rapidity distributions in the  $W^+ - N$  center of mass are being studied as a means of separating target from current fragmentation regions. One very exciting prospect is to use the Forward/Backward ratio of  $\Lambda^0$  production as a function of  $Q^2$  to set limits on the amount of higher twist contributions present. If a (dd) diquark in a neutron, rather than a single d quark, absorbs the weak current, the probability of forming a  $\Lambda^0$  or  $\Sigma^0$  in the forward  $W^+ N$  hemisphere will be enhanced, since the direction of the emitted (ud) diquark and the observed  $\Lambda^0$ 's are strongly correlated.

An attempt to analyze our results in terms of the percent of charm production and decay from the valence and sea quark targets is under way. The production of strange resonances  $K^*$  and  $Y^*$  is also being studied.

#### (5) Charm Production

For our charmed particle studies, about 80% of our film has now been analyzed for  $V^0$  events. After cuts used to obtain a clean sample of charged current events we have found 564  $K^0$ 's and 481  $\Lambda^0$ 's. The mass resolutions for  $K^0$ 's and  $\Lambda^0$ 's are 5.1 and 1.7 MeV respectively as shown in Fig.B4. We note that for the  $K^0$ 's, this is more than three times better than the resolution obtained from a neon experiment.

In an inclusive study of the final state combinations  $\Lambda\pi^+$ ,  $\Lambda\pi^+\pi^+\pi^-$ ,  $K^0p$ ,  $K^0p\pi^+\pi^-$ , we see evidence for the  $\Lambda_c^+$  charmed baryon at mass 2.28 GeV (to be submitted to Phys. Rev.) The results are shown in Fig.B5. For the D mesons we see a signal, Fig.B6, but it is clear we need more data.

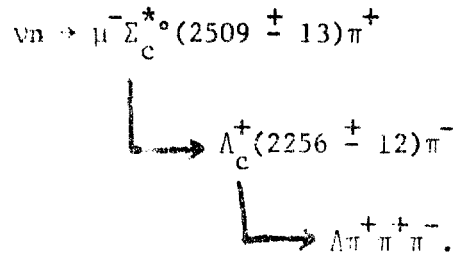
We have also had success in exclusive events which can be fit with  $V^0$ 's plus charged particles in the final state. Eleven candidates for charmed baryon events have been found, seven for  $\Lambda_c^+ \rightarrow \Lambda\pi^+$ , three for  $\Lambda_c^+ \rightarrow \Lambda\pi^+\pi^+\pi^-$  and one for  $\Lambda_c^+ \rightarrow K^0p$ .

Of the seven  $\Lambda_c^+ \rightarrow \Lambda\pi^+$  events two can be interpreted as  $\nu n \rightarrow \mu^- \Lambda_c^+$ . To confirm the  $\Lambda\pi^+$  events further, we show in Fig.B7 the  $\Lambda\pi^+$  mass distribution from events which have an exclusive fit for  $\Delta S = -1$  with a  $\Lambda$ . We find four excess events above background at the  $\Lambda_c^+$  mass. An increase in our data by a factor of  $\sim 2 - 3$  would give strong evidence for  $\Lambda_c$  production in exclusive reactions.

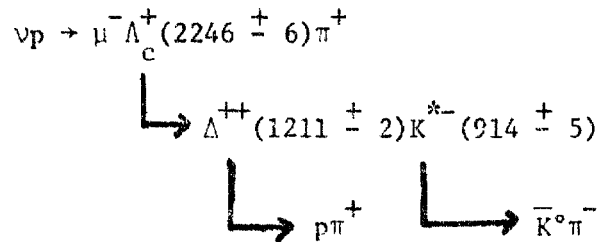
One event of three  $\Lambda_c^+ \rightarrow \Lambda\pi^+\pi^+\pi^-$  candidates is interpreted as  $\nu n \rightarrow \mu^- \Lambda_c^+$ . The two other events have five pions in the final state and can be fit to  $\nu n \rightarrow \mu^- \Lambda\pi^+\pi^+\pi^-\pi^-$ . The first can be interpreted as:

$$\begin{array}{l}
 \nu n \rightarrow \mu^- \Sigma_c^{++} (2486 \pm 19) \pi^- \\
 \quad \downarrow \\
 \quad \rightarrow \Lambda_c^+ (2257 \pm 17) \pi^+ \\
 \quad \quad \downarrow \\
 \quad \quad \rightarrow Y^{*-} (1382 \pm 3) \pi^+ \pi^+ \\
 \quad \quad \quad \downarrow \\
 \quad \quad \quad \rightarrow \Lambda\pi^-
 \end{array}$$

The second can be interpreted as



The  $\Lambda_c^+ \rightarrow K^0 p$  event is fit to  $\nu p \rightarrow \mu^- p \pi^+ K^0 \pi^- \pi^+$  and can be interpreted as



Further and more detailed analysis of both the inclusive and exclusive studies of charm production is underway.

#### (6) Hadron Multiplicity Distributions

We have examined the multiplicity distribution of the final state hadrons produced in charged current  $\nu p$  and  $\nu n$  interactions. In this discussion, all data are corrected for the effects of rescattering within the deuteron, as described in (1) above.

The hadron multiplicity distributions in  $\nu N$  scattering are observed to be similar to those in  $\bar{p}p$  annihilations, but systematic differences between neutrino-nucleon and hadron-nucleon multiplicity distributions are noted.

The average charged hadron multiplicity,  $\langle n_c \rangle$ , is observed to be a linear function of  $\ln W^2$ , where  $W$  is the total hadronic energy, for both  $\nu p$  and  $\nu n$  interactions. The variation of  $\langle n_c \rangle$  with  $W$  which we observe for

$\nu p$  interactions is consistent with that reported in two neutrino-hydrogen experiments,<sup>(3,4)</sup> while  $\langle n_c \rangle$  in  $\nu n$  interactions is systematically lower than the  $\nu p$  values by about half a unit.

The variation of the dispersion of the neutrino-nucleon multiplicity distribution may be parameterized by  $D = A \langle n_c \rangle + B$ . The value of the intercept  $B$  for  $\nu p$  interactions is found to be different from the value for  $\nu n$  interactions, although the slope parameter  $A$  is the same for the two targets. We find  $A = 0.34$  for neutrino-nucleon collisions, which is only 60% of the value of  $A$  for hadron-nucleon collisions. The result that the intercept  $B$  is non-zero is evidence that the data do not obey KNO scaling.

#### (7) Other Topics in the Hadronic Final States

A variety of problems concerning the final state hadrons are or will soon be under analysis and we expect interesting results within the coming months. We mainly list these topics here as it is still too early to give precise results. Recall that neutrinos provide a uniquely labelled source of quarks and diquarks whose fragmentation properties have been used to describe essentially all of hadron physics. More refined data along these lines for protons and neutrons are very useful for correlating a multitude of strong interaction observations.

##### a) QCD effects -

We are studying QCD effects which may be observed in final state distributions as well as in structure functions and their moments both

for neutrons and protons. Also, in preliminary studies we have found that the distribution of  $\langle p_T^2 \rangle$  as a function of  $W^2$  is consistent with QCD predictions. The differences of neutron and proton (n-p) fragmentation distributions are of particular theoretical interest.<sup>(5)</sup>

b) Jets -

An analysis of jet-like properties of final state particles in terms of the usual parameters of sphericity, spherocity, thrust, etc., is also being carried out.

c)  $\pi^-$  structure function -

By studying  $\nu n$  events in which a slow proton (not the spectator) is produced, one can effectively study  $\nu \pi^-$  scattering<sup>(6)</sup>. We are now beginning this analysis.

d) Charge flow and quark fragmentation -

Forward charge flow in the  $W^+ - N$  system is being studied along with questions of quark and diquark fragmentation and "leakage" between current and target fragmentation regions.

e) Resonance production -

Studies of production of baryon and meson resonances, both strange and non-strange are underway.

Additional topics slated for study are: comparison of  $\nu q$  with  $e q$  scattering, Adler sum rule tests, quasi-elastic  $\nu n \rightarrow \mu^- p$  scattering and exclusive reactions with  $V^0$ 's.

## REFERENCES

1. E.M. Riordan et al., SLAC-PUB-1634 (1975); A. Bodek et al., Phys. Rev. D20, 1471 (1979); W.B. Atwood, SLAC-PUB-185 (1975).
2. J. Steinberger, Particles and Fields Division Conference, Montreal, 1979; R.D. Field and R.P. Feynman, Phys. Rev. D15, 2590 (1977) and references therein.
3. J.W. Chapman et al., Phys. Rev. Lett. 36, 124 (1976).
4. ABCMO Collaboration, presented by H. Saarikko, Neutrino 79, Bergen, Norway.
5. G. Altarelli et al., Nucl. Phys. B160, 301 (1979).
6. M. Lusignoli et al., Nucl. Phys. B155, 394 (1979).
7. A.J. Buras and K.J.F. Gaemers, Nucl. Phys. B132, 249 (1979).

## FIGURE CAPTIONS

- Fig. B1. Bjorken  $x$  distributions for neutrino scattering on neutrons and protons. The fits shown are based on expressions from Buras and Gaemers.
- Fig. B2. The Feynman-Field fit to  $[\frac{d\sigma}{dx}(\nu n) - \frac{d\sigma}{dt}(\nu p)]_{CC}$ . The fit is normalized to the data at  $x = 0.14$ .
- Fig. B3. A preliminary result for the neutral current coupling constants  $u_L^2$  and  $d_L^2$ . Also shown is the prediction of the Weinberg-Salam model. Note that the  $\nu n$  line intersects the  $\nu p$  line at a greater angle than does the  $\nu(I=0)$  line (not shown) making this in principle a more sensitive method than previously used.
- Fig. B4. Mass distributions for  $K^0$  and  $\Lambda$  events yielding resolutions of 5.1 and 1.7 MeV respectively.
- Fig. B5. Inclusive mass distributions for (a)  $\Lambda\pi^+$ , (b)  $K^0p$ , and (c) their sum.
- Fig. B6. Inclusive mass distributions for (a)  $K^0\pi^+\pi^-$ , (b)  $K^0\pi^+ + K^0\pi^+\pi^+$ , and (c) their sum.
- Fig. B7. Mass distributions for  $\Lambda\pi^+$  from exclusive reactions fit with a single  $\Lambda$ . Also shown is the mass distribution for  $\Lambda\pi^+\pi^+$  from these reactions.

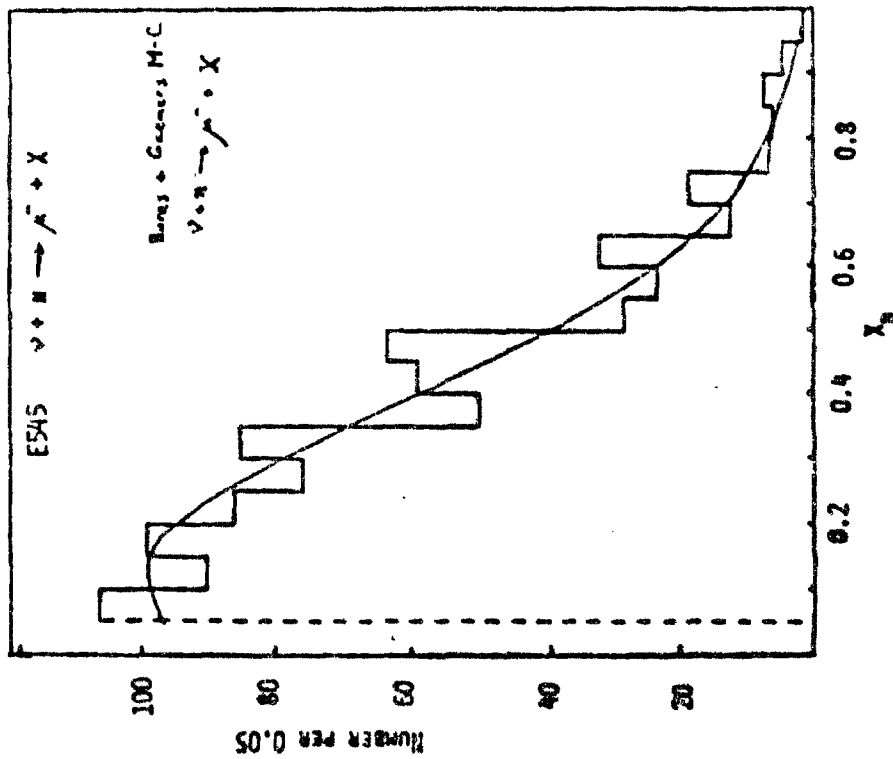
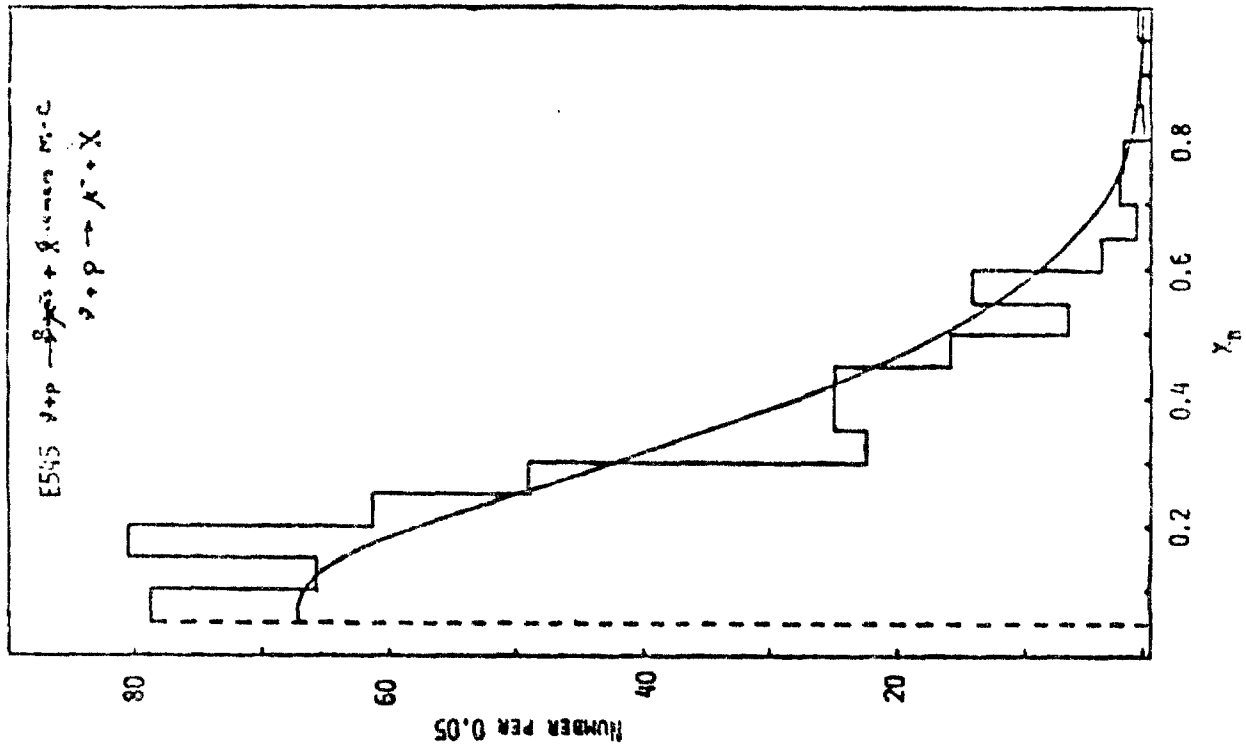


Figure B1

E-545: IIT- MD- SB- Tohoku - Tufts

$$\left[ \frac{d\sigma}{dx}(\nu n) - \frac{d\sigma}{dx}(\nu p) \right]_{C.C.}$$

$$\langle E_\nu \rangle \cong 55 \text{ GeV}$$

$$E_\nu > 15 \text{ GeV}$$

$$p_T > 1 \text{ GeV}/c$$

$$\Sigma p_\perp > 5 \text{ GeV}/c$$

$$(f_d = 0.094)$$

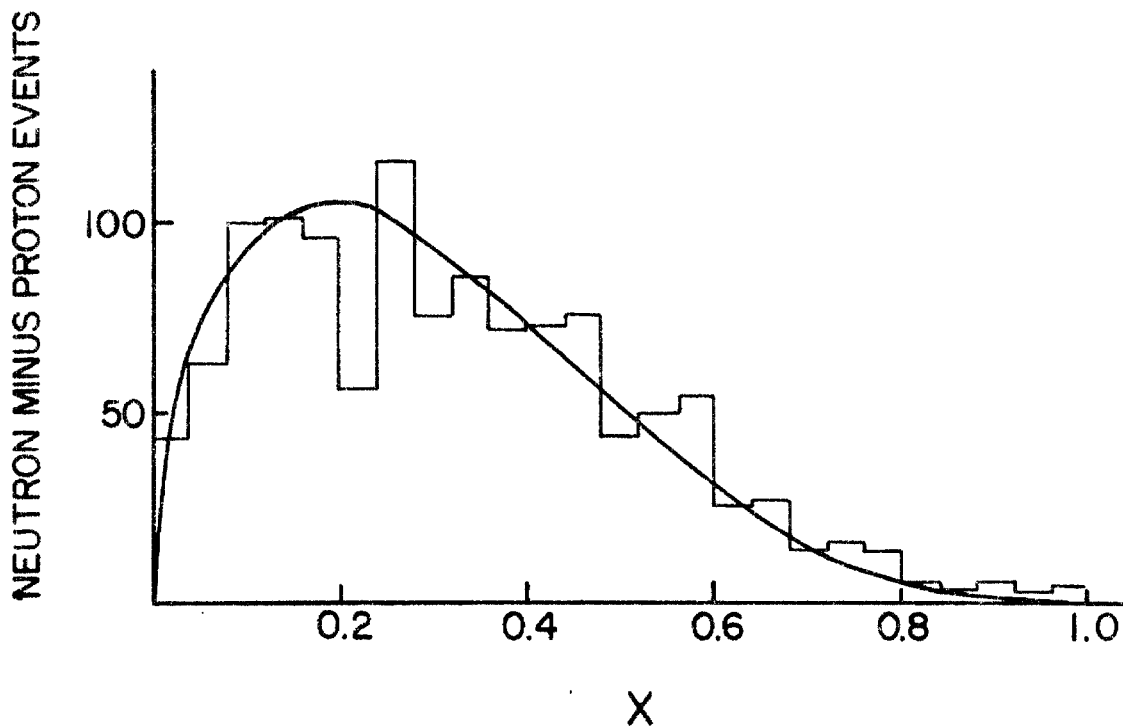


Figure B2

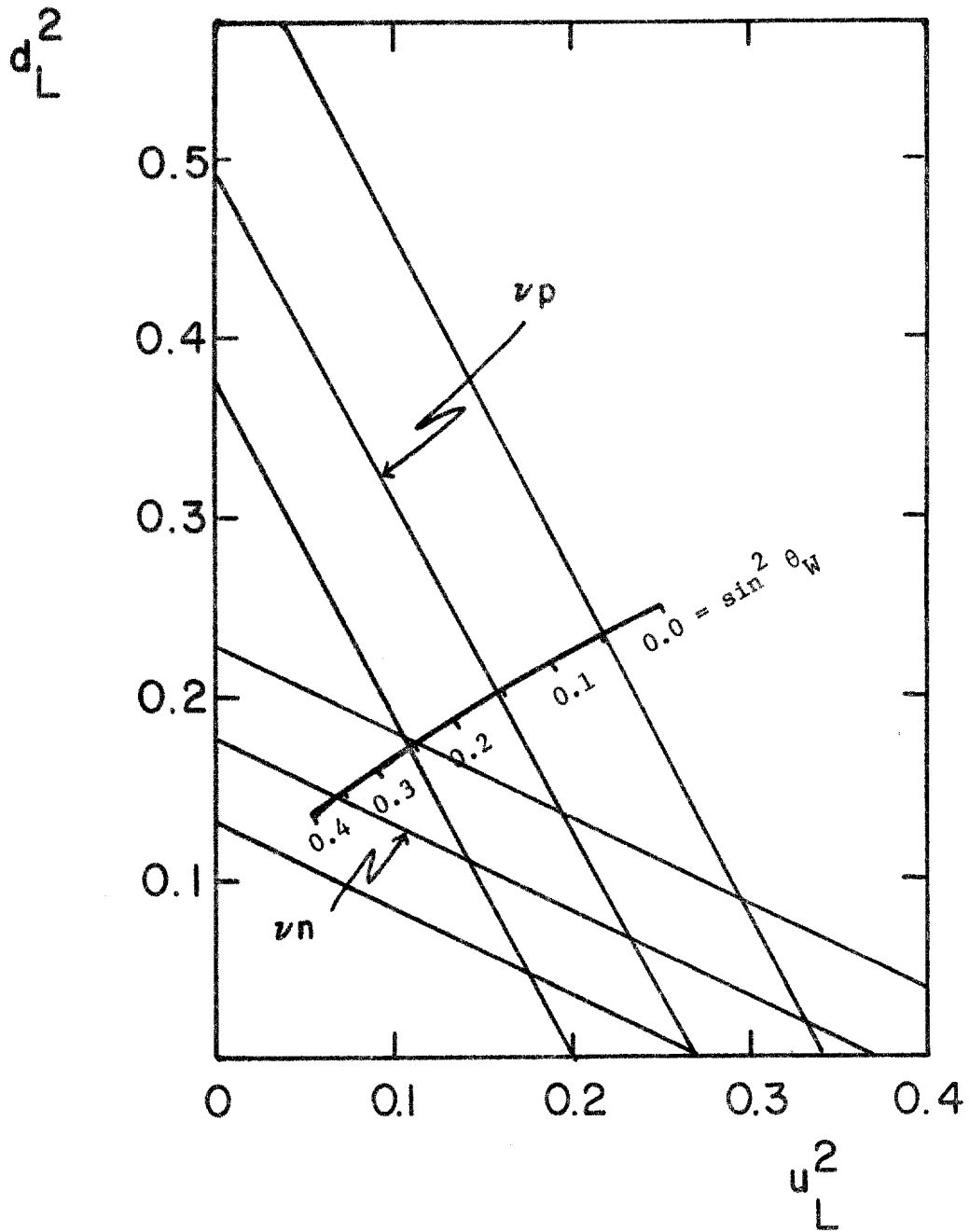


Figure B3

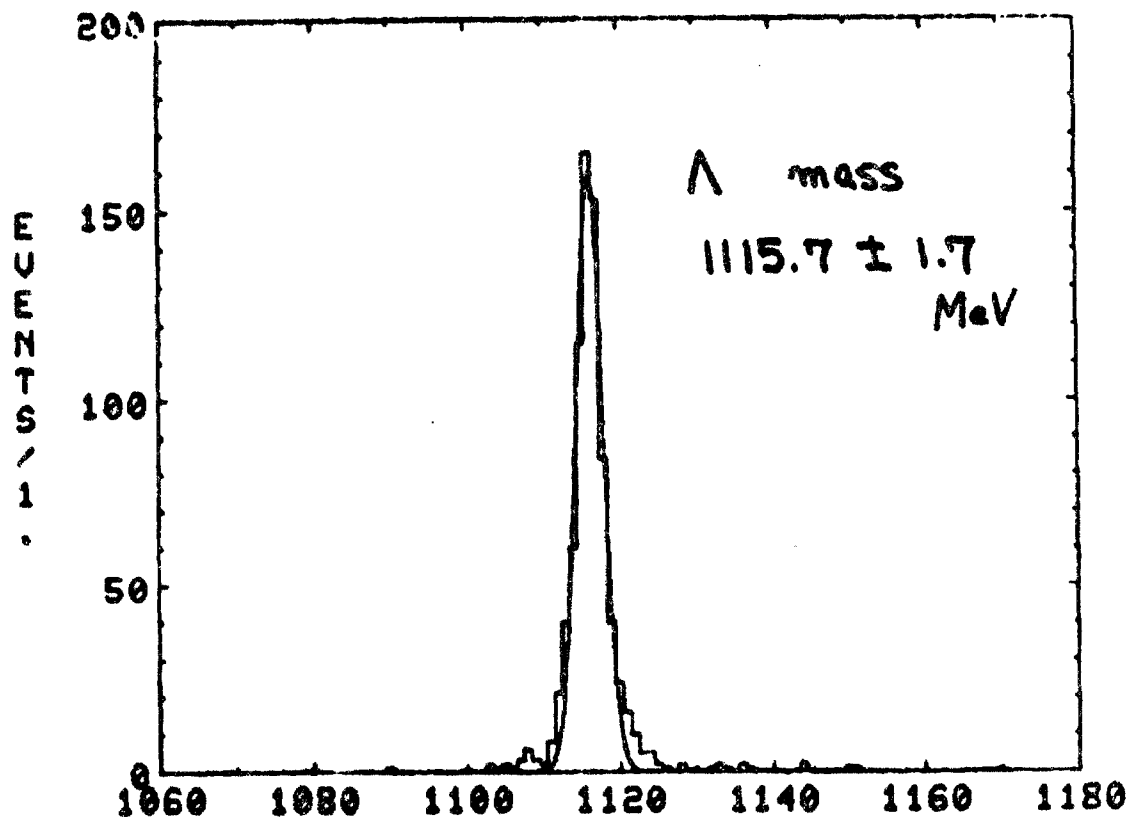
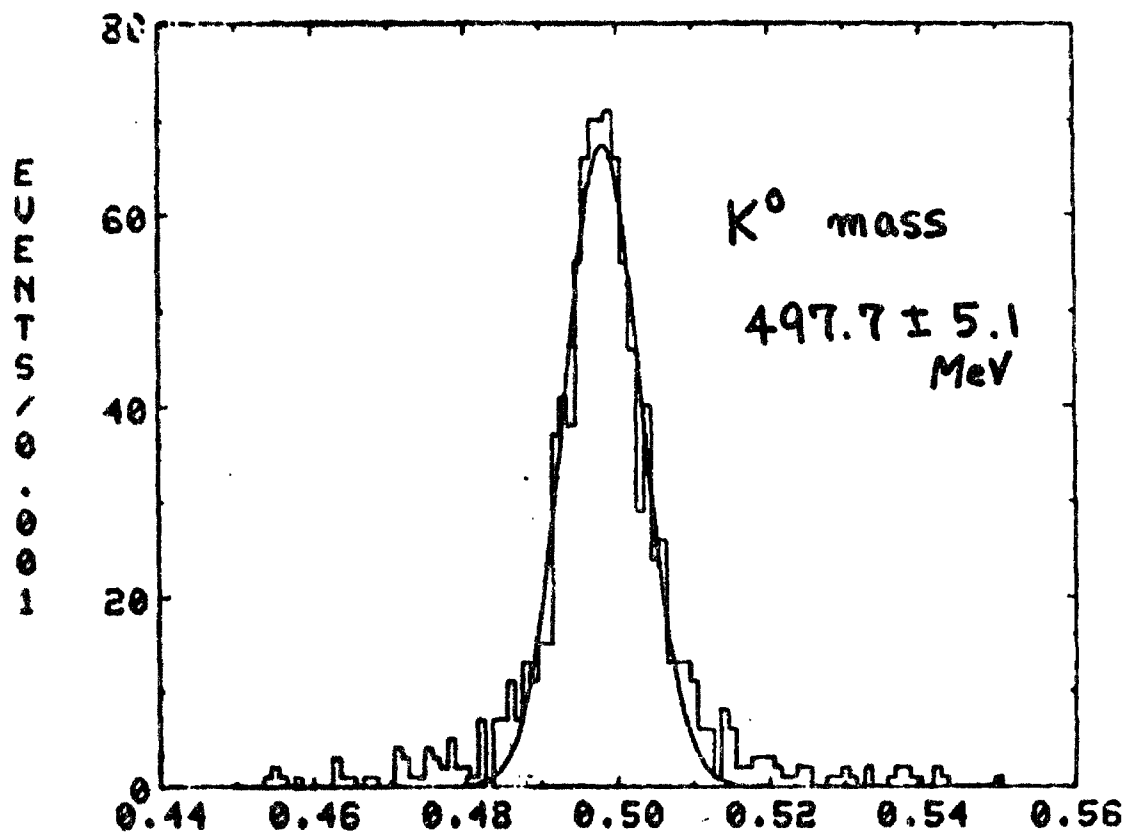


Figure B4

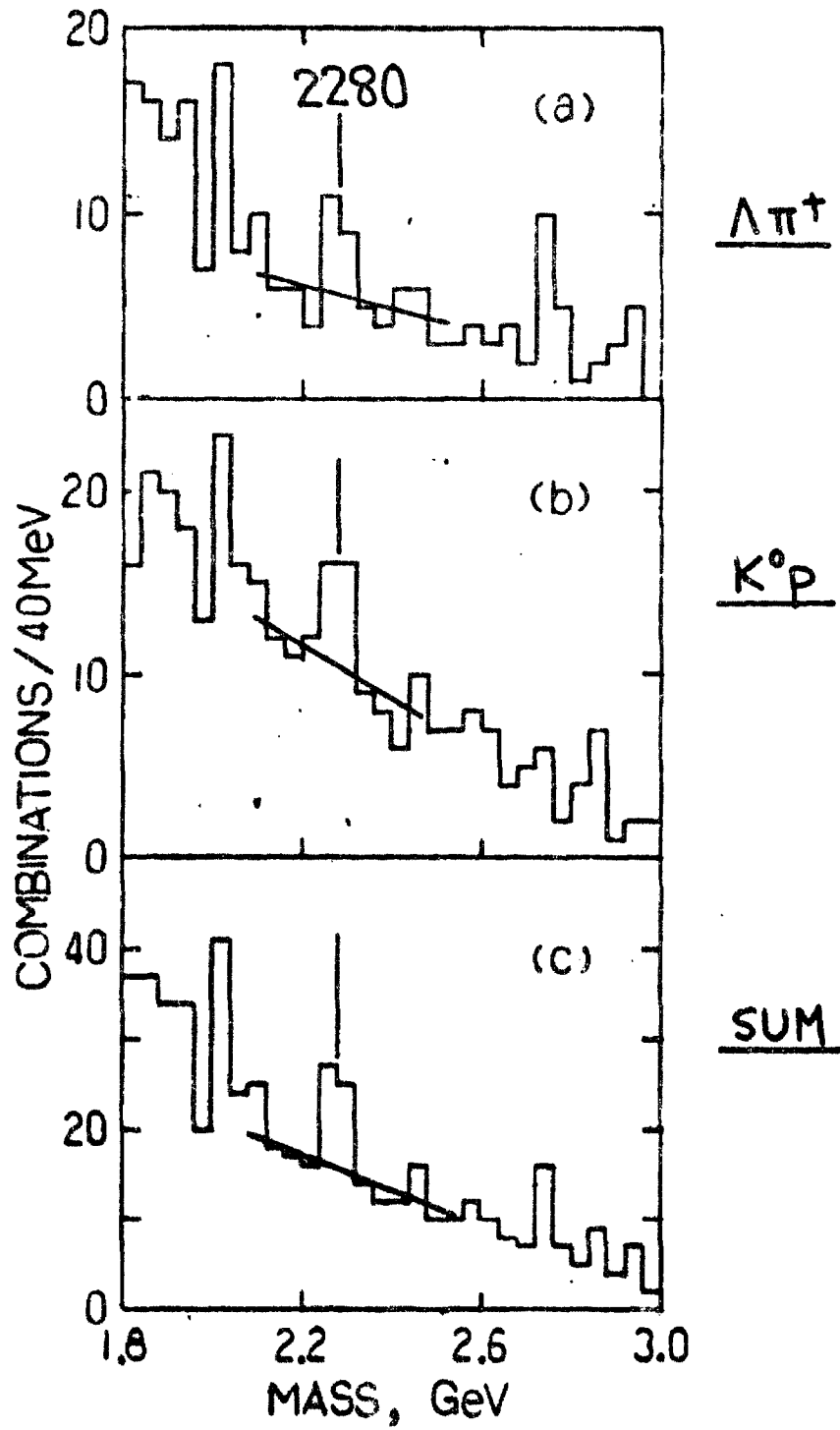


Figure B5

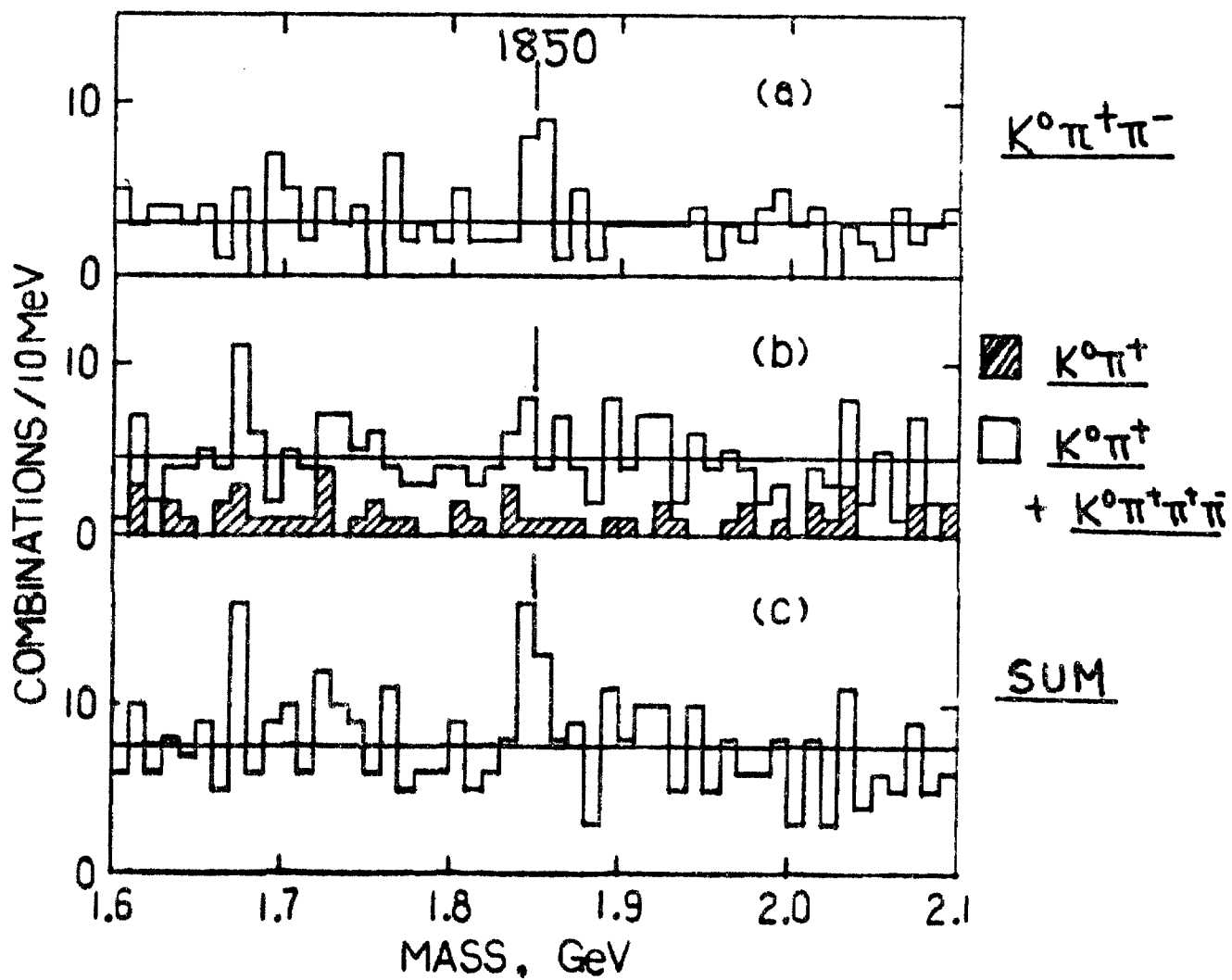


Figure B6

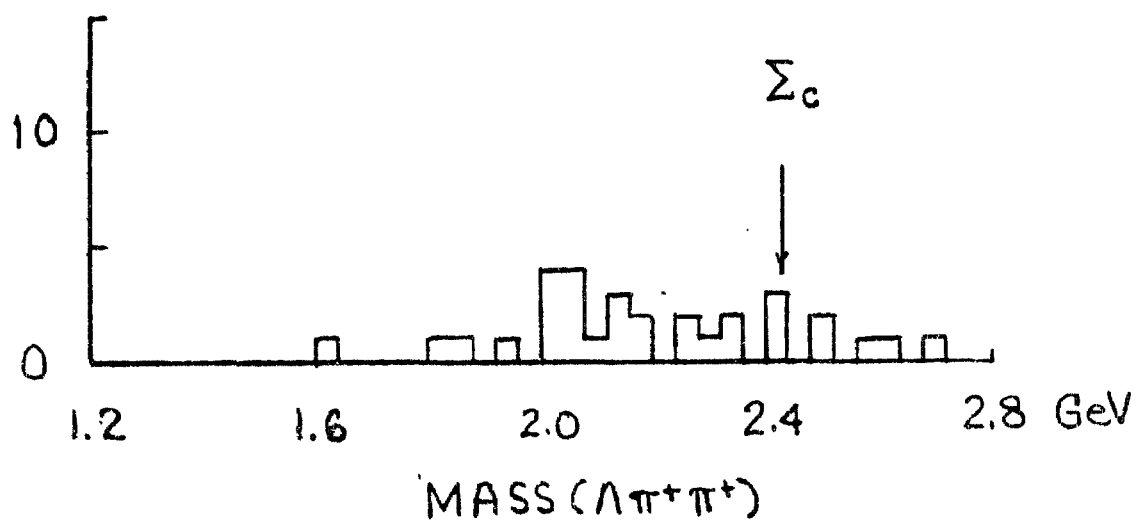
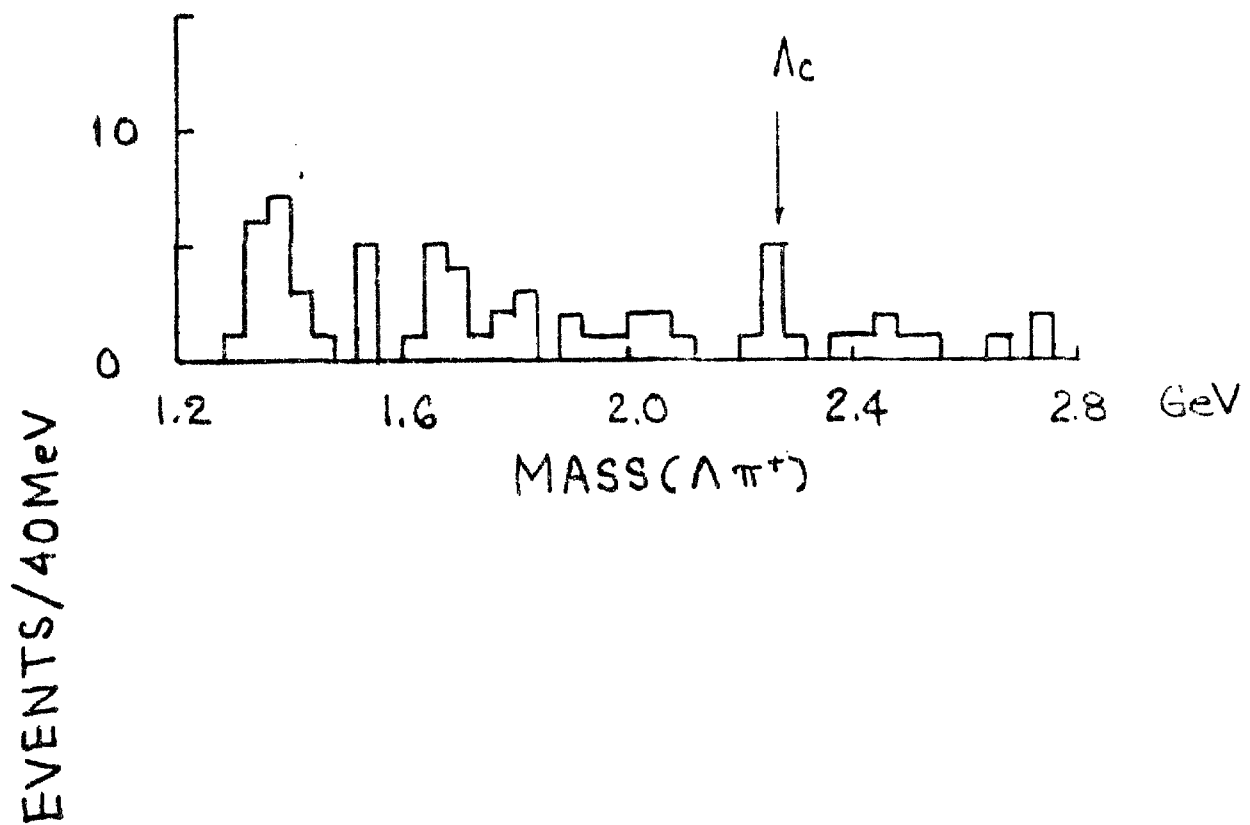
Exclusive Reactions ( $\Delta S = -1$ ) $E_\gamma > 5 \text{ GeV}$ 

Figure B7